# Continental-scale macro-fungal assemblage patterns correlate with climate, soil carbon and nitrogen deposition

Authors:

Carrie Andrew, Rune Halvorsen, Einar Heegaard, Thomas W Kuyper, Jacob Heilmann-Clausen, Irmgard Krisai-Greilhuber, Claus Bässler, Simon Egli, Alan C Gange, Klaus Høiland, Paul M Kirk, Beatrice Senn-Irlet, Lynne Boddy, Ulf Büntgen, Håvard Kauserud

Affiliations:

**CA** (corresponding author) (carrie.andrew@wsl.ch), Swiss Federal Research Institute WSL, CH-8903 Birmensdorf, Switzerland; (2nd affiliation:) University of Cambridge, Department of Geography, CB2 3EN, UK; (3rd affiliation:) Section for Genetics and Evolutionary Biology (EVOGENE), University of Oslo, Blindernveien 31, 0316 Oslo, Norway

**RH** (rune.halvorsen@nhm.uio.no), Department of Research and Collections, Natural History Museum, University of Oslo, NO-0318 Oslo, Norway

**EH** (fmroehe@fylkesmannen.no), Forestry and Forest Resources, Norwegian Institute of Bioeconomy Research, Fanaflaten 4, N-5244 Fana, Norway

**TWK** (thom.kuyper@wur.nl), Department of Soil Quality, Wageningen University, PO Box 47, 6700 AA Wageningen, The Netherlands

**JHC** (jheilmann-clausen@snm.ku.dk), Centre for Macroecology, Evolution and Climate, Natural History Museum of Denmark, University of Copenhagen, DK-2100 Copenhagen, Denmark

**IKG** (irmgard.greilhuber@univie.ac.at), Department of Botany and Biodiversity Research, University of Vienna, A-1030 Vienna, Austria

**CB** (Claus.Baessler@npv-bw.bayern.de), Bavarian Forest National Park, Freyunger Str. 2, D-94481 Grafenau, Germany; (2nd affiliation:) Technical University of Munich, Chair for Terrestrial Ecology, Hans-Carl-von-Carlowitz-Platz 2, 85354 Freising, Germany

**SE** (simon.egli@wsl.ch), Swiss Federal Research Institute WSL, CH-8903 Birmensdorf, Switzerland

**ACG** (a.gange@rhul.ac.uk), School of Biological Sciences, Royal Holloway, University of London, Egham, Surrey TW20 0EX, UK

**KH** (klaus.hoiland@ibv.uio.no), Section for Genetics and Evolutionary Biology (EVOGENE), University of Oslo, Blindernveien 31, 0316 Oslo, Norway

**PMK** (P.Kirk@kew.org), Mycology Section, Jodrell Laboratory, Royal Botanic Garden, Kew, Surrey TW9 3DS, UK

**BSI** (beatrice.senn@wsl.ch), Swiss Federal Research Institute WSL, CH-8903 Birmensdorf, Switzerland

**LB** (BoddyL@cardiff.ac.uk), School of Biosciences, Cardiff University, Sir Martin Evans Building, Museum Avenue, Cardiff CF10 3AX, UK

**UB** (ulf.buentgen@geog.cam.ac.uk), University of Cambridge, Department of Geography, CB2 3EN, UK; (second affiliation:) Swiss Federal Research Institute WSL, CH-8903 Birmensdorf, Switzerland; (third affiliation:) Global Change Research Centre and Masaryk University, 613 00 Brno, Czech Republic

**HK** (havard.kauserud@ibv.uio.no), Section for Genetics and Evolutionary Biology (EVOGENE), University of Oslo, Blindernveien 31, 0316 Oslo, Norway

Keywords (6-10): Assemblage, Biogeography, Climate, Ectomycorrhizal, Europe, Fungi, Macroecology, Saprotrophic, Temporal change

Running-title: Fungal assemblages across Europe

Abstract:

**Aim** Macroecological scales of species compositional trends are well documented for a variety of plant and animal groups, but remain sparse for fungi, despite their ecological importance in carbon and nutrient cycling. It is, thus, essential to understand the composition of fungal assemblages across broad geographical scales, and the underlying drivers. Our overall aim was to describe these patterns for fungi across two nutritional modes (saprotrophic and ectomycorrhizal). Furthermore, we aimed to elucidate the temporal component of fruiting patterns and to relate these to soil carbon and nitrogen deposition.

**Location** Central and northern Europe

**Methods** 4.9 million fungal fruit body observations throughout Europe, collected between 1970–2010, were analyzed to determine the two main environmental and geographical gradients structuring fungal assemblages for two main nutritional modes, saprotrophic and ectomycorrhizal fungi.

**Results** Two main gradients explaining the geography of compositional patterns were identified, for each nutritional mode. Mean annual temperature (and related collinear, seasonal measures) correlated most strongly with the first gradient for both nutritional modes. Soil organic carbon was the highest correlate of the second compositional gradient for ectomycorrhizal fungi, suspected as an indicator of vegetation- and pH-related covariates. In contrast, nitrogen deposition constituted a second gradient for saprotrophic fungi, likely a proxy for anthropogenic pollution. Compositional gradients and environmental conditions correlated similarly when the data were divided into two time intervals of 1970–1990 and 1991–2010. Evidence of compositional temporal change was highest with increasing altitude and latitude.

**Main conclusions** Fungal assemblage patterns demonstrate clear biogeographical patterns that relate the nutritional modes to their main environmental correlates of temperature, soil

organic carbon and nitrogen deposition. With respect to global change impacts, the highest rates of compositional change by time suggest targeting higher latitudes and altitudes for a better understanding of fungal dynamics. We, finally, suggest further examination of the ranges and dispersal abilities of fungi to better assess responses to global change.

Biosketch

Carrie Andrew has been responsible for preparing the manuscript, and for many of the analyses conducted with, the data utilized here, and as is better described in Andrew et al. 2017 (where original data sources and contact / website information are listed). Dr. Andrew was a postdoctoral researcher for the duration of this project. The work presented in this manuscript represents a component of the ClimFun project, an international collaboration that united national-scale fruit body datasets for the purposes of macroecological investigations of fungi in relation to environmental drivers, especially global change components. Author contributions are: HK, CA and EH, conceived the main ideas; CA prepared the data with data access and rights provided via ACG, BSI, CB, IKG, JHC, PMK, SE, and TWK; CA, RH and EH analysed the data; CA led the writing; and all co-authors contributed to wide-range general discussion and interpretation during the project, along with manuscript edits: RH, EH, TWK, JHC, IKG, CB, SE, ACG, KH, PMK, BSI, LB, UB, and HK.

Introduction

Detecting and understanding broad-scale geographic patterns of organisms is a critically important issue in global change research. Patterns of fungal species assemblage distributions have rarely been considered in macroecology, despite the key contributions that fungi make to ecosystem processes (Heilmann-Clausen, Barron, et al. 2014). There are two major functional guilds of fungi that produce macroscopic fruit bodies, based on nutritional mode (i.e., saprotrophic fungi that feed on dead organic matter, and ectomycorrhizal fungi that are mutualistic root symbionts), and each is crucial to ecosystem functioning. It is, thus, important to identify any differences in their geographic patterns, and changes in these, especially in relation to global change.

In terms of the known biogeographic patterns of fungi, mycorrhizal fungal species are strongly coupled to their host plants' ranges and climate regions (Tedersoo et al. 2012; Tedersoo, Bahram, Põlme, et al. 2014). Much research has focused on this connection, to the point of extrapolating biotic trends as a means to describe matching, un-surveyed fungal patterns (Soudzilovskaia et al. 2015; Swaty Michael, Deckert & Gehring 2016; Bueno et al. 2017). Saprotrophic fungi, also, are often considered in terms of their substrates, and their distribution often reflects the availability and quality of specific substrates, e.g., wood types and leaf litter (Bässler, Müller, Dziock & Brandl 2010; Heilmann-Clausen, Aude, et al. 2014). Gaps still exist in terms of knowledge of their overall distribution patterns, as well as the abiotic processes that likely determine their distributions.

The scattered representations of fungal biogeography studies to date have most often extrapolated low but sequence-deep sample intensities (small grain sizes) across large geographical extents, due to the limitations of molecular-based sampling approaches (Unterseher et al. 2011). This 'necessary evil' that leaves gaps in our knowledge of fungal distributions in space and time. The related fungal community gradients, then, are not continuously represented (due to low density of geographical samples) and, instead, capture categorical levels of what are actually continuous patterns of variation.

The taxonomic coverage across studies can also limit extrapolations. While sequences are identified to operational taxonomic units approximating species (Meiser, Bálint & Schmitt 2014; Taylor et al. 2014), studies have often focused on specific families or genera to benefit phylogenetic knowledge (i.e., Naff, Darcy & Schmidt 2013; Tedersoo, Bahram, Ryberg, et al. 2014). Other studies have focused on higher-level taxa of bacteria or fungi (Martiny et al. 2006). Although previous studies have suggested, expectedly, that fungal communities

arrange along environmental and geographical gradients, this pattern is yet to be clearly investigated.

In Europe, extensive fungal fruit body records have been catalogued at the largest spatiotemporal scales currently available (Andrew et al. 2017). While records with comprehensive sampling distributions that span multiple decades make it possible to investigate temporal changes of fungi related to climate, such data sets have so far mainly been used for studying phenology (e.g., Kauserud et al. 2008; Kauserud et al. 2010; Büntgen, Kauserud & Egli 2012; Kauserud et al. 2012; Boddy et al. 2014). The uniform coverage of fungal species data throughout a large part of their geographical extent (Andrew et al. 2017), when aggregated at appropriate spatial resolutions and across decades of time, sets this data source apart from molecular-based data. These data capture the entirety of fungal environmental and geographical gradients more completely than current molecular data, and in this respect, are ideal sources to better understand environmental correlates to fungal biogeography.

It is this large spatiotemporal range of multisource fungal records data collected in varied manners, combined with booming additions through citizen science projects (e.g., Halme, Heilmann-Clausen, Rämä, Kosonen & Kunttu 2012; Heilmann-Clausen, Barron, et al. 2014), that counteracts other limitations of fruit body data. Although the records focus almost exclusively on macro-fungi i.e., fungi that form conspicuous fruit bodies, both above and belowground, these include many of the ecologically most significant groups. For example, habitat preference in wood-decomposing fungi and the decay they cause are well, if not completely, captured with fruit body records (e.g., Heilmann-Clausen et al. 2016). While sporadic and ephemeral fruiting patterns of fungi can limit the accuracy of their

representation, the problem is minimized by compiling data across multiple years and at broader spatial resolutions than original point observations (Andrew et al. 2017). Finally, presence-only data for fruit bodies are the sole source of large-scale historical-to-contemporary records in mycology. Thus, fruit body records offer unique ecological information that may open up new insights into the effects of global change on fungi. Due to the high spatiotemporal resolution and extent, they serve as a foundation to build upon for biogeographical and macroecological research in mycology.

In this study, we use 4.9 million fruit body occurrences, extracted from a large-scale, European meta-database with more than 6 million fungal fruit body records (Andrew et al. 2017), to identify the major fungal biogeographic compositional patterns in Europe. For fungi in two main nutritional modes, saprotrophic and ectomycorrhizal, we first identified the gradients structuring assemblages and their environmental correlates. We next investigated differences in fungal compositional patterns between two equal time periods, 1970–1990 and 1991–2010, for each nutritional mode. In particular, we searched for geographical regions with greater compositional change, and for the overall environmental drivers that correlated with any compositional shift. As most knowledge in the field is untested, we adopted an inductive, hypothesis-generating approach, i.e., not to formulate specific hypotheses beyond a general expectation that the climate and environment (e.g., nitrogen deposition) that structures plant and fungal compositions at smaller scales will likely similarly structure macro-scale fungal assemblages. From our results, we generate biogeographical and macroecological hypotheses related to fungi, and suggest topics for further research.

## Methods

### Fungal data

This study utilized data from a component of the ClimFun 'meta-database,' a set of unified, multi-source data which originated from many, independent data repositories of fungal fruiting records across Europe (Andrew et al. 2017). The data are comprehensive in temporal and spatial coverage, extending decades into the past and covering a large geographic range of Europe. Given the large temporal and spatial coverage of the data, they are a reliable source for answering questions in macroecology. These data have been shown to be especially robust to large-scale phenology analyses (Andrew et al. 2018), demonstrating their potential for biogeographical studies such as here. Earlier bias removal techniques included harmonization of nomenclature, removal of out-of-country records, removal of data with inconsistent or incomplete date records, removal of duplicate records, and other techniques standard for formatting these types of data formatting. Due to the large amount of records, these processes did not greatly affect the overall, final amounts (e.g., Andrew et al. 2017).

National-scale data in the ClimFun meta-database with a substantial amount of records (i.e., Austria, Denmark, Germany, Netherlands, Norway, Slovenia, Switzerland, and the United Kingdom) were selected across a timespan from 1970 to 2010, for which data were more reliable due to less recording bias than earlier time periods, and also was temporally robust, ensuring stability in climate values (as opposed to interannual weather variability). Species were restricted to the macroscopic fruit body forming Agaricomycotina (the classes Agaricomycetes, Tremellomycetes and Dacrymycetes; including fungi with flattened fruit bodies on wood and soil (corticoid fungi)), as other taxonomic groups comprised very low proportions of the records (Andrew et al. 2017) and, at this spatiotemporal scale, were highly biased in terms of under-collection and sampling bias. Taxa were assigned to their dominant nutritional mode based on Rinaldi, Comandini & Kuyper (2008), Tedersoo and Smith (2013), and with additional species-specific information added through expertise (nutritional mode

data compiled 2016 by K. Høiland, University of Oslo, Norway, with additional aid from: B. Senn-Irlet, J. Heilmann-Clausen, A. C. Gange, L. Boddy, S. Egli, T. W. Kuyper, I. Krisai-Greilhuber). The number of records varied between nutritional modes, as did the grid cell representation for each guild (see all results figures to compare between time period amounts and nutritional modes), with greater coverage by saprotrophic fungi.

Environmental data

Available environmental variables were gridded at the 50 × 50 km level after connecting the ClimFun records data in earlier steps to open-source metadata at their highest available resolutions (i.e., geographical points), thus gaining the most precision possible in terms of fruiting records and their associated environment. Environmental data were obtained and formatted from each of the following open-data sources: Climate and altitude data were extracted at the 2.5 and 0.5 minute resolution, respectively (equivalent to approximately 4.5 and 1 km at the equator), from WorldClim (http://www.worldclim.org; Hijmans, Cameron, Parra, Jones & Jarvis 2005). GIMMS AVHRR Global NDVI-3g (Normalized Difference Vegetation Index) data with 1/12-degree resolution (approximately 9.5 km at the equator) was extracted from Ecocast (https://ecocast.arc.nasa.gov). The average of annual averages of monthly mean value concatenated climate data composites for the period 1982–2010 was used. NDVI corresponds to the start of spring in northern latitudes and is thus often used as a measure of initial primary productivity (Pettorelli et al. 2005; Nielsen et al. 2012). Percent soil organic carbon was extracted from the OCTOP (Topsoil Organic Carbon Content for Europe) dataset, from the Joint Research Centre - European Soil Data Centre (ESDAC), with 1 km original resolution (http://esdac.jrc.ec.europa.eu/content/octop-topsoil-organic-carbon-content-europe). Reduced and oxidised nitrogen deposition data were obtained from Greenhouse Gas Management in European land use systems (GHG Europe) FP7, using 0.25

degree (approximately 27-28 km at the equator) NCAR CTM data (http://www.europe-fluxdata.eu/ghg-europe/data/others-data). Finally, land cover was extracted from the European Environment Agency (EEA) Corine Land Cover (CLC) 2006 raster data (version 17) with an original 100 m resolution (http://www.eea.europa.eu/data-and-maps/data/corine-land-cover-2006-raster-3). While data with varying spatial resolutions is not ideal, this issue was balanced against utilizing data with the best temporal resolution matching the fungal recordings, as well as the ability to find and extract data for each covariate.

To minimize multicollinearity, pairwise Pearson correlation coefficients between all potential environmental covariates were calculated (Appendix S1) and variables with a coefficient below a threshold of 0.60 (absolute value) were retained (cf. Dormann et al. 2013). Total and seasonal precipitation were positively correlated, as were annual, seasonal and ranges in temperature. In the case of temperature, the latter two were positively correlated with easting (longitude) and were thus not retained. Nitrogen deposition (both $NH_x$, and $NO_y$) was correlated with northing (negative) and easting (positive). $NH_x$ was selected for further analyses, serving also as a proxy for $NO_y$, with which it was strongly correlated. NDVI was correlated with northing and easting, but was retained as it is a more direct measure of seasonal primary productivity than northing or easting. Thus, nine variables were used in the analyses (Appendix S1; Figure 1): six environmental variables (mean annual temperature, summed annual precipitation, $NH_x$, soil percent organic carbon, NDVI, and dominating land-cover class) and three geographical variables (northing, easting and altitude). While these selected variables vary along gradients on the broad scales that are addressed in our study, it should be noted that correlative relationships do not imply causal relationships.

Data preparation

Fungal species records per latitude-longitude coordinate were summed within each 50 × 50 km grid extending over Europe and matched to UTM (Universal Transverse Mercator coordinate system; a more geographically accurate projection for both northing and easting bounds) zone 32. Environmental data were extracted for each fungal record (to precise latitude-longitude positions), and were then averaged within each grid cell to match the gridded fungal data. Land cover was recorded as the CLC class with the highest number of fungal records in each grid cell. Values for each environmental variable were originally linked directly to each species record at the most precise spatial resolution possible; thus, the values reported for grid cells are means for all data points found within each cell and not an overall equal-area average across each grid cell. They are optimally predictive of environmental conditions leading to a fruit body presence. Data were originally analysed at three spatial resolutions (50 × 50 km, 20 × 20 km and 10 × 10 km), with the 50 × 50 km resolution the one that best captured large-scale compositional dynamics while being least subject to spatial bias (Araújo, Thuiller, Williams & Reginster 2005). Geographical variables were represented by the value of the grid cell center point.

To understand temporal effects on compositional dynamics, for all taxa combined, as well as saprotrophic and ectomycorrhizal taxa separately, the fungal data were analyzed for the whole timespan (1970–2010) as well as for two time periods (split equally into 1970–1990 and 1991–2010). To help reduce collector biases in species representation, grid cells (grids) with less than a total of 499 records, summed across all fungal species, were removed from the whole time-period data set. Grids cells with less than a total of 249 records, summed across all fungal species in the earlier time period, were removed, as were those lacking records across both time periods. The impact of the value chosen for the minimum amount of records within grid cells (249) was analysed during model optimization. Similar model results, or less

optimal models, were obtained with number of records per grid cells of less than 4999, 2499, 999, and 249 summed records per grid (half these values for the two-time periods). The influence of rare species was clear in grids when those with only less than 2 summed records were removed (and inappropriate for analysis). The influence of abundantly fruiting species was minimized by collapsing records to single units per geographical location (i.e., record duplications were removed), though our data are populated by rarer to abundantly fruiting taxa; hence the need for studies across fungal tissue and methodological types."

Statistical analyses

To summarize the main gradient structure of fungal assemblage compositions, Global Non-metric Multidimensional Scaling (GNMDS) and Detrended Correspondence Analysis (DCA) ordinations were obtained in accordance with the multiple parallel ordination approach of van Son and Halvorsen (2014, and references therein), using the vegan (Oksanen et al. 2013) and MASS (Venables and Ripley 2002) packages in R. By this procedure, only ordination axes that are extracted by both methods were accepted as important compositional gradients, thereby ensuring that spurious axes (which may occasionally be produced by any ordination method; Økland 1996) were not subjected to further interpretation. Many combinations of data properties, settings, and options for the methods were explored in the initial phase of the data analyses, including: counts, relative counts and frequencies as measures of species' abundances in the grid cells; combined with the whole- as well as the two-time period datasets; as well as for all, saprotrophic and ectomycorrhizal subsets of fungal communities. GNMDS analyses with count data utilized the Bray-Curtis dissimilarity index while the Jaccard index was used for frequency data. Each of the following settings were applied to the count data, and the first three to relative count and frequency data, during GNMDS analyses: no transformations or standardizations (absolute values were used), geodesic transformation,

Hellinger standardization, power transformation, and Wisconsin double-standardization. For further interpretation, DCA with power-function transformed count data was selected. The axes of these DCA's were confirmed by GNMDS by calculating pairwise correlation coefficients between the axes. Between the models, axis 1 correlations ranged from 0.74–0.93 while axis 2 ranged from 0.23–0.82, with lowest correlation between ectomycorrhizal and saprotrophic groups.

Ordination results were visualized by plotting DCA axis scores on the positions of each grid cell. The difference between ordination scores for each of the two axes and for the two time periods was used as the response variable in an analysis of temporal change patterns. Kendall's non-parametric correlation coefficient $\tau$ was used to assess the significance of environmental components in explaining community variability as represented by the DCA axes (Supplemental Table 2). Variables that strongly correlated with one or both of the first two DCA axes were fitted to the ordination diagram using linear regression and displayed as either linear-termed fixed effects or cubic smooth splines (Økland 1996; Tenenbaum, De Silva & Langford 2000; Wood 2006; Mahecha, Martínez, Lischeid & Beck 2007; Liu et al. 2008). The categorical land cover variable was analysed with the function envfit in vegan and was found always to be significant (data not shown). The function also verified significance of the Kendall's tau correlations for all other variables. Absolute values of $\tau > 0.30$ were considered substantially correlated with a DCA axis while $\tau$ values in the interval 0.20–0.30 were considered as marginal.

The statistical significance of the temporal difference in fungal species composition (originating from one DCA) was assessed by three methods: paired t-tests of the individual DCA axes scores; a multivariate paired Hotelling's T-squared test for the axes differences

with respect to time period; and a principal component analysis (PCA) on the matrix of compositional change. Further PCA analyses with proportions rejected a concern that compositional change was due to sampling bias between the two time periods. As results were all complementary, DCA score differences were selected to be plotted geographically as a demonstration of compositional change between the time intervals.

While not emphasized, as our goals concerned determining how the biogeography of fungal assemblages related to environmental gradients, we did determine the potential that any temporal changes in fungal assemblages were mostly the result of specific species' changes by time (see supplemental material). Indicator species analyses were conducted on the results of the DCA scores for each of the two time intervals, utilizing the difference in scores between the first and second time periods for the response matrix. The species were divided into groups by positive, negative or relatively little (no; between -0.1275–0.1275 for saprotrophic and -0.0625–0.0625 for ectomycorrhizal groups) DCA axis score change between the time periods. The groups were created by separating scores into equal components of DCA score matching the color coding for figures created. Analysis was conducted with the indicspecies package. All data formatting and analyses were implemented in R version 3.2.2.

## Results

The primary gradients of saprotrophic and ectomycorrhizal fungal species assemblages were both correlated with mean annual temperature (Figures 2a and 3a; Appendix S2); Kendall's $\tau$ values were –0.55 for saprotrophic and –0.48 for ectomycorrhizal fungi. The highest correlations for each group were for temperatures linked to cold-season measures (coldest month or coldest quarter). Grid cells at the geographical and temperature extremes (the

Norwegian and Alp mountain ranges) were similar with high DCA axis 1 scores, most clearly seen for the saprotrophic fungi. In contrast, grid cells from western, coastal and low-lying parts of Europe occurred along the opposite, low-score DCA axis 1 gradient.

The second compositional gradient (DCA axis 2) differed between nutritional modes. For saprotrophic assemblages, the gradient reflected patterns related to nitrogen deposition levels ($\tau = -0.49$; Figure 2b). DCA axis 2 scores increased from central Europe to coastal areas of the UK and Norway, which matched general nitrogen patterns (Figure 1e). In contrast, the second assemblage gradient for ectomycorrhizal fungi separated assemblages of grid cells from northern to central Europe (Figure 3b) and was correlated with soil organic carbon content ($\tau = 0.36$) (Figure 1c). The entire fungal community reflected similar patterns to the saprotrophic fungi (Appendix S3; Appendix S2) and is thus not discussed further.

When separated into two time periods (1970–1990 and 1991–2010), patterns reflected those described for the whole time period. Temperature was again the main correlate along the primary gradient identified for saprotrophic ($\tau = -0.51$) and ectomycorrhizal ($\tau = -0.38$) fungal assemblages (Figure 4), with cold-season temperatures also showing high correlations (Appendix S2). Patterns reflected those described for the whole time period. As with the whole time period, saprotrophic fungal assemblages were separated along a second gradient related to NHx ($\tau = -0.37$), and ectomycorrhizal fungal assemblages along a gradient related to soil organic carbon ($\tau = 0.37$) and mean annual temperature ($\tau = -0.43$).

The saprotrophic fungal assemblage gradients correlated with temperature (axis 1) and nitrogen (axis 2). For both of the gradients, the greatest DCA score change was for grid cells situated to the north and at higher altitudes, i.e., in the Norwegian mountain region (Figure 4

a, b). For the first, temperature-related gradient, a pattern of change was found in the opposite direction in at least some regions of the Alps mountain range of Switzerland and Austria. There were no robust indicator species for any of the DCA axis change groups in terms of specificity (probability of a group based on a species' presence) and fidelity (probability of finding a species in a group), though many species matched high specificity values (Appendix S4). Nitrogen was similarly strongly correlated with DCA scores along the second gradient (Appendix S2), with areas of lower nitrogen amounts tending to occupy either extreme along the gradient. Areas in central and western Europe exhibited the least amount of temporal change along both gradients. Though the number of grid cells was fewer for ectomycorrhizal fungi, there was a similar trend of greatest temporal differences in assemblages at the highest latitudes and altitudes (Figure 4 c, d). No highly matched indicator species were found for any group, though as with the saprotrophic fungi, many species contained high specificity values but very low fidelity values (Appendix S5).

## Discussion

Assemblage gradients for both saprotrophic and ectomycorrhizal fungi correlated with mean annual temperature (and collinear, cold-season temperature measures), which, as expected, were patterned by geography and altitude. Assemblages with higher mean annual temperatures were more similar to each other than to those at lower temperatures (Figures 2 and 3 a, c, e). Most notably, the composition of fungal assemblages in mountainous regions were similar, regardless of whether they were situated in Norway or the Alps region of Switzerland and Austria. If we were able to conduct the same analyses at a more precise spatial scale that could incorporate vegetation data into the models, we expect that, in line with earlier studies, we would find a significant relationship between the fungal and environmental gradients, as identified with respect to fungal composition gradients, with

vegetation type (e.g., Tedersoo et al. 2012; Soudzilovskaia et al. 2015; Swaty et al. 2016; Bueno et al. 2017). A clear next challenge is to connect the fungal-environment relationships to the fungal-vegetation relationships, ideally while simultaneously separating direct and indirect effects from each other.

The second main assemblage gradient (DCA axis 2) was both different in its pattern and varied in the main environmental correlate between the nutritional modes, though it was relatively uniform in terms of geographic and altitudinal distribution (Figures 2 and 3 b, d, e). The saprotrophs displayed assemblage patterns related to a gradient of N deposition, which itself reflected oceanicity-continentality patterning, and which is a likely proxy for anthropogenic impacts on the environment. The ectomycorrhizal pattern related to soil organic carbon and was less geographically structured, though similar to that found by Gange et al. (2017) in the UK. While our results cannot determine causation, different feeding strategies may explain the correlation of nitrogen with saprotrophic fungal assemblages, and soil organic carbon (SOC) with ectomycorrhizal fungal assemblages (Appendix S2).

Ectomycorrhizal fungal roles in carbon sequestration and cycling are increasingly recognized, especially in northern latitude forests (Clemmensen et al. 2013; Averill and Hawkes 2016; Kyaschenko, Clemmensen, Karltun & Lindahl 2017). The high correlation we found between an assemblage composition gradient (the 2$^{nd}$ DCA axis) and SOC content suggests that ectomycorrhizal fungi not only respond to, but also causally contribute to processes of organic matter accumulation and, hence, carbon sequestration (Figure 1c, f). We effectively captured the distributional gradation of basidiomycete taxa by vegetation type from acidic, carbon-rich northern bogs and fens of the UK, transitioning to ectomycorrhizal dominance in northern and mountainous forests of Scandinavia and the Alps region of Switzerland and

Austria, on predominantly mor soils. Those locations can be contrasted with the more continental pasturelands and woodlands containing either less woody plants or forests with different ectomycorrhizal fungal communities and soil types. Soil pH, which is often highly correlated with turnover in fungal community composition (Rineau and Garbaye 2009) and implicated in fungal biogeography (Tedersoo, Bahram, Põlme, et al. 2014), is strongly, negatively correlated with SOC content at a European scale (Bueno et al. 2017). SOC can also be considered as an inverse proxy of pH. This second main compositional gradient signifies the importance of carbon and structurally-bound compounds (and non-measured determinants of soil carbon, e.g., vegetation and soil pH), as well as any consequential potential changes (related to climate or land-use change) to fungi and their ecosystem services.

Neither of the two most important ectomycorrhizal compositional gradients were strongly correlated with nitrogen deposition amounts (a correlation of $\tau = -0.23$ was found for the second DCA axis; Appendix S2), which might at a first glance be surprising because effects of N deposition on ectomycorrhizal fungal communities have been well established (Arnolds 1991; Lilleskov, Fahey & Lovett 2001; Peter, Ayer & Egli 2001; Avis, McLaughlin, Dentinger & Reich 2003). We suggest two main explanations for this discrepancy of our results with those of others: First, a weaker correlation means that the assemblage gradients were structured more strongly by other factors, i.e., temperature and soil carbon, rather than nitrogen deposition *per se*. Accordingly, our results are compatible with a considerable effect of nitrogen deposition on fungi, but suggest interactions with carbon sequestration that have also been shown experimentally (de Vries et al. 2009). Alternatively, the second time span (1991–2010) might have reduced visible N impacts on assemblages, as nitrogen pollution especially started to abate from 1994 onwards (van Strien, Boomsluiter, Noordeloos, Verweij & Kuyper 2017). This is in accord with the reduction of N that has recently taken place in the

Netherlands, which has caused a marked rebound by once-affected ectomycorrhizal taxa, especially those considered nitrogen-sensitive (nitrophobic) (van Strien et al. 2017). A manipulative experiment testing the abatement of longer-term nitrogen addition similarly demonstrated a re-convergence to greater community similarity with non-nitrogen enriched treatments than those with persistent nitrogen addition (Andrew C. and Avis P., unpublished data). Temporally dynamic environmental variables, when available, would be of further assistance in clarifying responses, as would careful inspection between regions.

Interestingly, while saprotrophic fungi typically are less documented and, thus, generally thought to exhibit less sensitivity to nitrogen deposition, the second compositional gradient was highly correlated with nitrogen deposition (Figure 2 b, d, e). Studies of nitrogen addition effects on saprotrophs have, however, pinpointed wood decay fungi as being susceptible (Allison, Hanson & Treseder 2007). Community impacts of elevated nitrogen level have also previously been found (Allison et al. 2009), though muted compared to our own results. The molecular-based approach by those authors, covering a broader taxonomic range (at a far smaller spatial scale), include many more taxa of the Ascomycota which, compared to macro-fungi, are likely to be less susceptible to N. Thus, the focus on Basidiomycota and the inclusion of wood decaying fungi in our macro-fungal data set may explain the more pronounced community response to large-scale N content (Figure 1e). Nitrogen was also significantly correlated with community structure when analysed across the two time intervals (Appendix S2). Our results suggest that saprotrophic macro-fungi are an important group to focus on in terms of nitrogen effects, with certain groups more sensitive than even ectomycorrhizal fungi. The marginal correlation with precipitation ($\tau = 0.27$) should be further explored, as it likely represents a community gradient that reflects a response to oceanic vs. continental climates.

Fungal assemblage composition varied with time, but only in certain regions and with a magnitude that varied in relation to the environmental covariates (Figure 4). The more dramatic temperature range shift by elevation (compared to latitude), and consequent assemblage change, appears to match the distributional patterns of plant species ranges (Halbritter, Alexander, Edwards & Billeter 2013) and mirrors bioclimatic zonation related to temperature (annual temperature, length of growing season). Our results indicate that fungal assemblages in European mountain ranges are more similar, across large geographic distances, than with those of the lowlands. This may be due to similarities in land-cover type (Figure 1f), hosts or climatic factors themselves. Elevation structured communities differently by latitude, for both saprotrophic and ectomycorrhizal fungi, supporting the suggestion that the indirect effects of latitude and altitude cannot be assumed similar even if both are structured by temperature (Halbritter et al. 2013; Grytnes et al. 2014), which also directly affects organisms. Other factors can contribute independently to differences between each mountain range, e.g., slope steepness, precipitation (Engler et al. 2011), and components of biotic interactions (Pellissier et al. 2013), and could explain some of the discrepancies in assemblage gradient changes. Relating dispersal to range shifts would also help clarify responses (Siefert, Lesser & Fridley 2015).

Greater change in assemblages occurred with saprotrophic than ectomycorrhizal fungi, evidenced by a wider range in the difference of DCA axes scores between time periods (Figure 4). More marked temporal-based changes in phenological responses by saprotrophic fungi have also consistently been found, suggesting that these fungi may respond more rapidly than ectomycorrhizal fungi, and in a variety of ways, i.e., by compositional as well as phenological changes (Kauserud et al. 2012; Andrew et al. 2018). It would be of ecological

interest to quantify the extent to which the latter is a direct cause of the former. The degree to which greater saprotrophic temporal change is related to management practices, forest stand succession, or other global change components also requires further study (Bässler et al. 2010; Nordén et al. 2013; Heilmann-Clausen, Aude, et al. 2014). The effects of management might require, however, a more precise scale resolution than that used in the current, broad-scale study.

Our results may serve as a platform for further macroecological research on fungi. For example, the abiotic and biotic components of the most clearly defining biogeographical gradients should be further examined, especially in relation to global change. We suggest priority be given to biogeographical relationships of variables that act upon fungi in a direct way, i.e., temperature and moisture, given how they non-additively structured fungal assemblages, especially in terms of latitude and altitude. As mentioned earlier, it is imperative to better connect fungi, plants and the environment, as science currently relies too often on two-way relationships rather than a network approach capable of addressing all three main components. Similarly, we must understand how fungal ranges, at large scales, are distributed relative to one another as well as with respect to their hosts and/or substrates. Finally, as we report on macro-fungal fruit bodies (as a proxy for understanding fungal assemblage patterns overall), a primary role of which are related to reproduction and dispersal of fungi, we suggest that adding in information on long-distance dispersal abilities – be it via spores, vegetative structures, host or animal vectors – will help clarify the potential for movement of fungi into new and changing habitats. These suggestions all lead to consideration of the potential for further change of fungal communities under future global change scenarios, and what the ecological relevance might then be.

Acknowledgements

Two sources are acknowledged for financial support: The Research Council of Norway, project “Climate change impacts on the fungal ecosystem component (ClimFun)” (11 of 38 months), and the Swiss National Science Foundation, project "Linking European Fungal Ecology with Climate Variability” (11 months). Drs. Dag Endresen, Vegar Bakkestuen, and Anders Nielsen we thank for open-source data acquisition. As always, our appreciation to employees and volunteers that over the years collected, managed and provided rights to the fungal data: the Austrian Mycological Society and Wolfgang Dämon; the Swiss national database (www.swissfungi.ch) and Peter Jakob; Deutsche Gesellschaft für Mykologie (German Mycological Society) and Dr. Martin Schmidt; The Danish Fungal Atlas project and Tobias Frøslev, Thomas Læssøe, Jens. H. Petersen and Jan Vesterholt; the Netherlands Mycological Society (NMV) and A. van den Berg; the Mycological Herbarium at the Natural History Museum (University of Oslo); the Slovenian Forestry Institute, the Central database of fungi in Slovenia, the Slovenian Mycological Association, and Dr. Nikica Ogris; www.fieldmycology.net for support sources of the UK national database. We also acknowledge critical and constructive comments of the editor and three anonymous reviewers.

Data availability: All fungal and associated meta-data are provided as used for analyses in this study and are gridded at the 50 × 50 km resolution. Please see the included information on original sources of data, or else the methods and acknowledgments sections of this manuscript.

References

Allison, S.D., Hanson, C.A. & Treseder, K.K. (2007). Nitrogen fertilization reduces diversity and alters community structure of active fungi in boreal ecosystems. *Soil Biology and Biochemistry*, 39, 1878-1887.

Allison, S.D., LeBauer, D.S., Ofrecio, M.R., Reyes, R., Ta, A.M. & Tran, T.M. (2009). Low levels of nitrogen addition stimulate decomposition by boreal forest fungi. *Soil Biology and Biochemistry*, 41, 293-302.

Andrew, C., Heegaard, E., Kirk, P.M., Bässler, C., Heilmann-Clausen, J., Krisai-Greilhuber, I.,… Kauserud, H. (2017). Big data integration: Pan-European fungal species observations assembly that addresses contemporary questions in ecology and global change biology. *Fungal Biology Reviews*, 31, 88-98.

Andrew, C., Heegaard, C., Gange, A.C., Senn-Irlet, B., Egli, S., Kirk, P.M.,… Boddy, L. (2018). Congruency in fungal phenology patterns across dataset sources and scales. *Fungal Ecology*, 32, 9-17.

Araújo, M.B., Thuiller, W., Williams, P.H., & Reginster, I. (2005). Downscaling European species atlas distributions to a finer resolution: implications for conservation planning. *Global Ecology and Biogeography*, 14, 17-30.

Arnolds, E.E.F. (1991). Decline of ectomycorrhizal fungi in Europe. *Agriculture, Ecosystems & Environment*, 35, 209-244.

Averill, C., & Hawkes, C.V. (2016). Ectomycorrhizal fungi slow soil carbon cycling. *Ecology Letters*, 19, 937-947.

Avis, P.G., McLaughlin, D.J., Dentinger, B.C., & Reich, P.B. (2003). Long-term increase in nitrogen supply alters above-and below-ground ectomycorrhizal communities and increases the dominance of Russula spp. in a temperate oak savanna. *New Phytologist*, 160, 239-253.

Boddy, L., Büntgen, U., Egli, S., Gange, A.C., Heegaard, E., Kirk, P.M.,… Kauserud, H. (2014). Climate variation effects on fungal fruiting. *Fungal Ecology*, 10, 20-33.

Bueno, C.G., Moora, M., Gerz, M., Davison, J., Öpik, M., Pärtel, M.,… Zobel, M. (2017). Plant mycorrhizal status, but not type, shifts with latitude and elevation in Europe. *Global Ecology and Biogeography*, 26, 690-699.

Bässler, C., Müller, J., Dziock, F., & Brandl, R. (2010). Effects of resource availability and climate on the diversity of wood-decaying fungi. *Journal of Ecology*, 98, 822-832.

Büntgen, U., Kauserud, H., & Egli, S. (2012). Linking climate variability to mushroom productivity and phenology. *Frontiers in Ecology and the Environment*, 10, 14-19.

Clemmensen, K.E., Bahr, A., Ovaskainen, O., Dahlberg, A., Ekblad, A., Wallander, H.,… Lindahl, B.D. (2013). Roots and associated fungi drive long-term carbon sequestration in boreal forest. *Science*, 339, 1615-1618.

de Vries, W., Solberg, S., Dobbertin, M., Sterba, H., Laubhann, D., Van Oijen, M.,… Reinds, G.J. (2009). The impact of nitrogen deposition on carbon sequestration by European forests and heathlands. *Forest Ecology and Management*, 258, 1814-1823.

Dormann, C.F., Elith, J., Bacher, S., Buchmann, C., Carl, G., Carré, G.,… Münkemüller, T. (2013). Collinearity: a review of methods to deal with it and a simulation study evaluating their performance. *Ecography*, 36, 27-46.

Engler, R., Randin, C.F., Thuiller, W., Dullinger, S., Zimmermann, N.E., Araújo, M.B.,… Choler, P. (2011). 21st century climate change threatens mountain flora unequally across Europe. *Global Change Biology*, 17, 2330-2341.

Gange, A.C., Heegaard, E., Boddy, L., Andrew, C., Kirk, P., Halvorsen, R.,… Kauserud, H. (2017). Trait-dependent distributional shifts in fruiting of common British fungi. *Ecography*. *40*, doi: 10.1111/ecog.03233

Grytnes, J.A., Kapfer, J., Jurasinski, G., Birks, H.H., Henriksen, H., Klanderud, K.,… Birks, H.J.B. (2014). Identifying the driving factors behind observed elevational range shifts on European mountains. *Global Ecology and Biogeography*, 23, 876-884.

Halbritter, A.H., Alexander, J.M., Edwards, P.J., & Billeter, R. (2013). How comparable are species distributions along elevational and latitudinal climate gradients? *Global Ecology and Biogeography*, 22, 1228-1237.

Halme, P., Heilmann-Clausen, J., Rämä, T., Kosonen, T., & Kunttu, P. (2012). Monitoring fungal biodiversity–towards an integrated approach. *Fungal Ecology*, 5, 750-758.

Heilmann-Clausen, J., Barron, E.S., Boddy, L., Dahlberg, A., Griffith, G.W., Nordén, J.,… Halme, P. (2014). A fungal perspective on conservation biology. *Conservation Biology*, 29, 61-68.

Heilmann-Clausen, J., Aude, E., Dort, K., Christensen, M., Piltaver, A., Veerkamp, M.,… Òdor, P. (2014). Communities of wood-inhabiting bryophytes and fungi on dead beech logs in Europe–reflecting substrate quality or shaped by climate and forest conditions? *Journal of Biogeography*, 41, 2269-2282.

Heilmann-Clausen, J., Maruyama, P.K., Bruun, H.H., Dimitrov, D., Læssøe, T., Frøslev, T.G., & Dalsgaard, B. (2016). Citizen science data reveal ecological, historical and evolutionary factors shaping interactions between woody hosts and wood-inhabiting fungi. *New Phytologist*, 212, 1072-1082.

Hijmans, R.J., Cameron, S.E., Parra, J.L., Jones, P.G., & Jarvis, A. (2005). Very high resolution interpolated climate surfaces for global land areas. *International journal of Climatology*, 25, 1965-1978.

Kauserud, H., Stige, L.C., Vik, J.O., Økland, R.H., Høiland, K., & Stenseth, N.C. (2008). Mushroom fruiting and climate change. *Proceedings of the National Academy of Sciences*, 105, 3811-3814.

649 Kauserud, H., Heegaard, E., Semenov, M.A., Boddy, L., Halvorsen, R., Stige, L.C.,…
650 Stenseth, N.C. (2010). Climate change and spring-fruiting fungi. *Proceedings of the Royal*
651 *Society of London B: Biological Sciences*, 277, 1169-1177.
652
653 Kauserud, H., Heegaard, E., Büntgen, U., Halvorsen, R., Egli, S., Senn-Irlet,… Høiland, K.
654 (2012). Warming-induced shift in European mushroom fruiting phenology. *Proceedings of*
655 *the National Academy of Sciences*, 109, 14488-14493.
656
657 Kyaschenko, J., Clemmensen, K.E., Karltun, E., & Lindahl, B.D. (2017). Below-ground
658 organic matter accumulation along a boreal forest fertility gradient relates to guild interaction
659 within fungal communities. *Ecology Letters*, 20, 1546–1555
660
661 Lilleskov, E.A., Fahey, T.J., & Lovett, G.M. (2001). Ectomycorrhizal fungal aboveground
662 community change over an atmospheric nitrogen deposition gradient. *Ecological*
663 *Applications*, 11, 397-410.
664
665 Liu, H.Y., Økland, T., Halvorsen, R., Gao, J.X., Liu, Q.R., Eilertsen, O., & Bratli, H. (2008).
666 Gradient analyses of forests ground vegetation and its relationships to environmental
667 variables in five subtropical forest areas, S and SW China. *Sommerfeltia*, 32, 1e196.
668
669 Mahecha, M.D., Martínez, A., Lischeid, G., & Beck, E. (2007). Nonlinear dimensionality
670 reduction: alternative ordination approaches for extracting and visualizing biodiversity
671 patterns in tropical montane forest vegetation data. *Ecological Informatics*, 2, 138e149.
672

673 Martiny, J.B.H., Bohannan, B.J., Brown, J.H., Colwell, R.K., Fuhrman, J.A., Green, J.L.,…
674 Staley, J.T. (2006). Microbial biogeography: putting microorganisms on the map. *Nature*
675 *Reviews Microbiology*, 4, 102-112.
676
677 Meiser, A., Bálint, M., & Schmitt, I. (2014). Meta-analysis of deep-sequenced fungal
678 communities indicates limited taxon sharing between studies and the presence of
679 biogeographic patterns. *New Phytologist*, 201, 623-635.
680
681 Naff, C.S., Darcy, J.L., & Schmidt, S.K. (2013). Phylogeny and biogeography of an
682 uncultured clade of snow chytrids. *Environmental Microbiology*, 15, 2672-2680.
683
684 Nielsen, A., Yoccoz, N.G., Steinheim, G., Storvik, G.O., Rekdal, Y., Angeloff, M.,…
685 Mysterud, A. (2012). Are responses of herbivores to environmental variability spatially
686 consistent in alpine ecosystems?. *Global Change Biology*, 18, 3050-3062.
687
688 Nordén, J., Penttilä, R., Siitonen, J., Tomppo, E., & Ovaskainen, O. (2013). Specialist species
689 of wood-inhabiting fungi struggle while generalists thrive in fragmented boreal forests.
690 *Journal of Ecology*, 101, 701-712.
691
692 Oksanen, J., Blanchet, F.G., Kindt, R., Legendre, P., Minchin, P.R., O'Hara, R.B.,
693 Simpson, G.L., Solymos, P., Stevens, M.H.H., & Wagner, H. (2013). Vegan: Community
694 Ecology Package. R Package Version 2.0-9. http://CRAN.R-project.org/ package1⁄4vegan.
695

Pellissier, L., Pinto-Figueroa, E., Niculita-Hirzel, H., Moora, M., Villard, L., Goudet, J.,… Guisan, A. (2013). Plant species distributions along environmental gradients: do belowground interactions with fungi matter? *Frontiers in Plant Science*, 4, 500.

Peter, M., Ayer, F., & Egli, S. (2001). Nitrogen addition in a Norway spruce stand altered macromycete sporocarp production and below-ground ectomycorrhizal species composition. *New Phytologist*, 149, 311-325.

Pettorelli, N., Vik, J.O., Mysterud, A., Gaillard, J.M., Tucker, C.J., & Stenseth, N.C. (2005). Using the satellite-derived NDVI to assess ecological responses to environmental change. *Trends in Ecology & Evolution*, 20, 503-510.

Rinaldi, A.C., Comandini, O., & Kuyper, T.W. (2008). Ectomycorrhizal fungal diversity: seperating the wheat from the chaff. *Fungal Diversity*, 33, 1-45.

Rineau, F., & Garbaye, J. (2009). Effects of liming on ectomycorrhizal community structure in relation to soil horizons and tree hosts. *Fungal Ecology*, *2*, 103-109.

Siefert, A., Lesser, M.R., & Fridley, J.D. (2015). How do climate and dispersal traits limit ranges of tree species along latitudinal and elevational gradients? *Global Ecology and Biogeography*, 24, 581-593.

Soudzilovskaia, N.A., Douma, J.C., Akhmetzhanova, A.A., Bodegom, P.M., Cornwell, W.K., Moens, E.J.,… Cornelissen, J.H. (2015). Global patterns of plant root colonization intensity

by mycorrhizal fungi explained by climate and soil chemistry. *Global Ecology and Biogeography*, 24, 371-382.

Swaty, R., Michael, H.M., Deckert, R., & Gehring, C.A. (2016). Mapping the potential mycorrhizal associations of the conterminous United States of America. *Fungal Ecology*, 24, 139-147.

Taylor, D.L., Hollingsworth, T.N., McFarland, J.W., Lennon, N.J., Nusbaum, C., & Ruess, R.W. (2014). A first comprehensive census of fungi in soil reveals both hyperdiversity and fine-scale niche partitioning. *Ecological Monographs*, 84, 3-20.

Tedersoo, L., Bahram, M., Toots, M., Diedhiou, A.G., Henkel, T.W., Kjøller, R.,… Polme, S. (2012). Towards global patterns in the diversity and community structure of ectomycorrhizal fungi. *Molecular Ecology*, 21, 4160-4170.

Tedersoo, L., & Smith, M.E. (2013). Lineages of ectomycorrhizal fungi revisited: foraging strategies and novel lineages revealed by sequences from belowground. *Fungal Biology Reviews*, 27, 83-99.

Tedersoo, L., Bahram, M., Ryberg, M., Otsing, E., Kõljalg, U., & Abarenkov, K. (2014). Global biogeography of the ectomycorrhizal/sebacina lineage (Fungi, Sebacinales) as revealed from comparative phylogenetic analyses. *Molecular Ecology*, 23, 4168-4183.

Tedersoo, L., Bahram, M., Põlme, S., Kõljalg, U., Yorou, N.S., Wijesundera, R,… Abarenkov, K. (2014). Global diversity and geography of soil fungi. *Science*, 346, 1256688.

Tenenbaum, J.B., De Silva, V., & Langford, J.C. (2000). A global geometric framework for nonlinear dimensionality reduction. *Science*, 290, 2319e2323.

Unterseher, M., Jumpponen, A.R.I., Oepik, M., Tedersoo, L., Moora, M., Dormann, C.F., & Schnittler, M. (2011). Species abundance distributions and richness estimations in fungal metagenomics–lessons learned from community ecology. *Molecular Ecology*, 20, 275-285.

van Son T.C., & Halvorsen R. (2014). Multiple parallel ordinations: the importance of choice of ordination method and weighting of species abundance data. *Sommerfeltia*, 37, 1-37.

van Strien, A.J., Boomsluiter, M., Noordeloos, M.E., Verweij, R.J., & Kuyper, T.W. (2017). Woodland ectomycorrhizal fungi benefit from large-scale reduction of nitrogen deposition in the Netherlands. *Journal of Applied Ecology*, 55, 290-298.

Venables, W.N., & Ripley, B.D. (2002). Modern Applied Statistics with S, fourth ed. Springer, New York.

Wood, S.N. (2006). Generalized Additive Models, an Introduction with R. Chapmann and Hall, London.

Økland, R.H. (1996). Are ordination and constrained ordination alternative or complementary strategies in general ecological studies? *Journal of Vegetation Science,* 7, 289e292.

Figures legends

Figure 1: Environmental covariate gridded maps displaying mean values, by geo-coordinates linked to amount of fruit body records, for (a) mean annual temperature (degrees C), (b) averaged total precipitation per year (mm), (c) mean percent soil organic carbon, (d) mean NDVI, where lower values are less productive, (e) mean ammonia(-um) levels, NHx (kg N $m^{-2}$ $s^{-1}$ * $10^{-12}$), (f) land cover class (CLC 1), and (g) mean altitude (msl).

Figure 2: Gradients in the composition of saprotrophic fungal communities, their biogeographical distributions, and environmental correlates. Compositional similarities are represented by DCA axis 1 (a, c) and axis 2 (b, d) gradients mapped onto 50x50 km grids. Shading reflects DCA axis gradients, centered at zero (white), with darker values at either extreme. DCA plots (e) demonstrate the influence of mean annual temperature, altitude and nitrogen (NHx), all of which were highly correlated with either of the DCA axes.

Figure 3: Gradients in the composition of ectomycorrhizal fungal communities, their biogeographical distributions, and environmental correlates. Compositional similarities are represented by DCA axis 1 (a, c) and axis 2 (b, d) gradients mapped onto 50 × 50 km grids. Shading reflects DCA axis gradients, centered at zero (white), with darker values at either extreme. DCA plots (e) demonstrate the influence of mean annual temperature, altitude and percent soil organic carbon, all of which were highly correlated with either of the DCA axes.

Figure 4: Saprotrophic (a, b) and ectomycorrhizal (c, d) fungal community differences between two time periods (1970-1990 vs. 1991-2010). The temporal differences of communities by the two main DCA gradients ($t_2 - t_1$) are shown mapped. All point shadings

792 are centered at zero (coloured white), with shading reflecting DCA axis gradients of darker

793 values at either extreme.

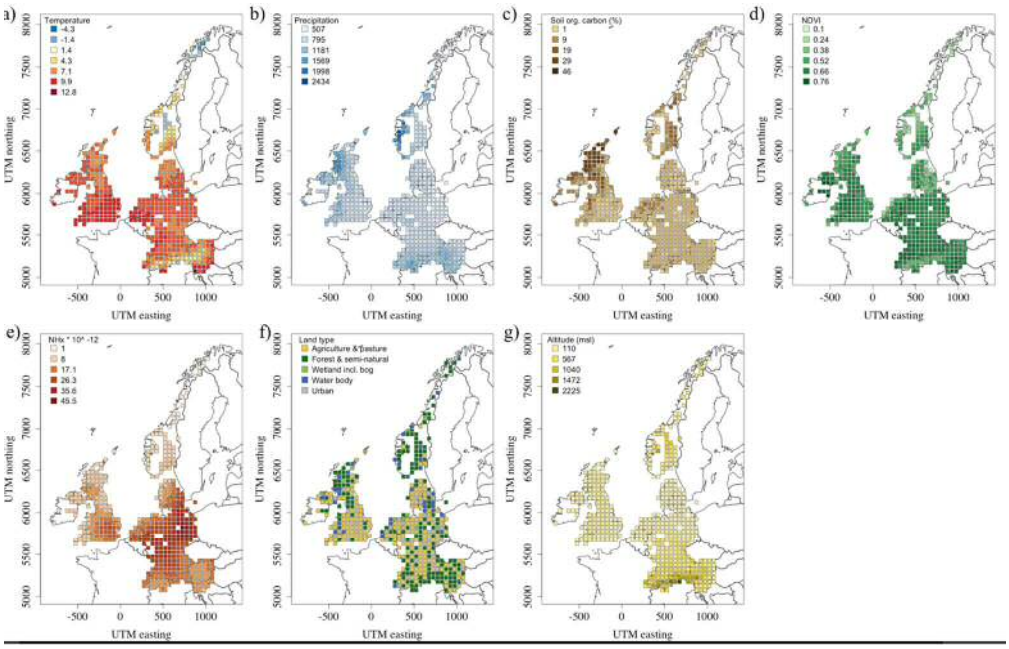


Environmental covariate gridded maps displaying mean values, by geo-coordinates linked to amount of fruit body records, for (a) mean annual temperature (degrees C), (b) averaged total precipitation per year (mm), (c) mean percent soil organic carbon, (d) mean NDVI, where lower values are less productive, (e) mean ammonia(-um) levels, NHx (kg N m-2 s-1 * 10-12), (f) land cover class (CLC 1), and (g) mean altitude (msl).

243x155mm (160 x 160 DPI)

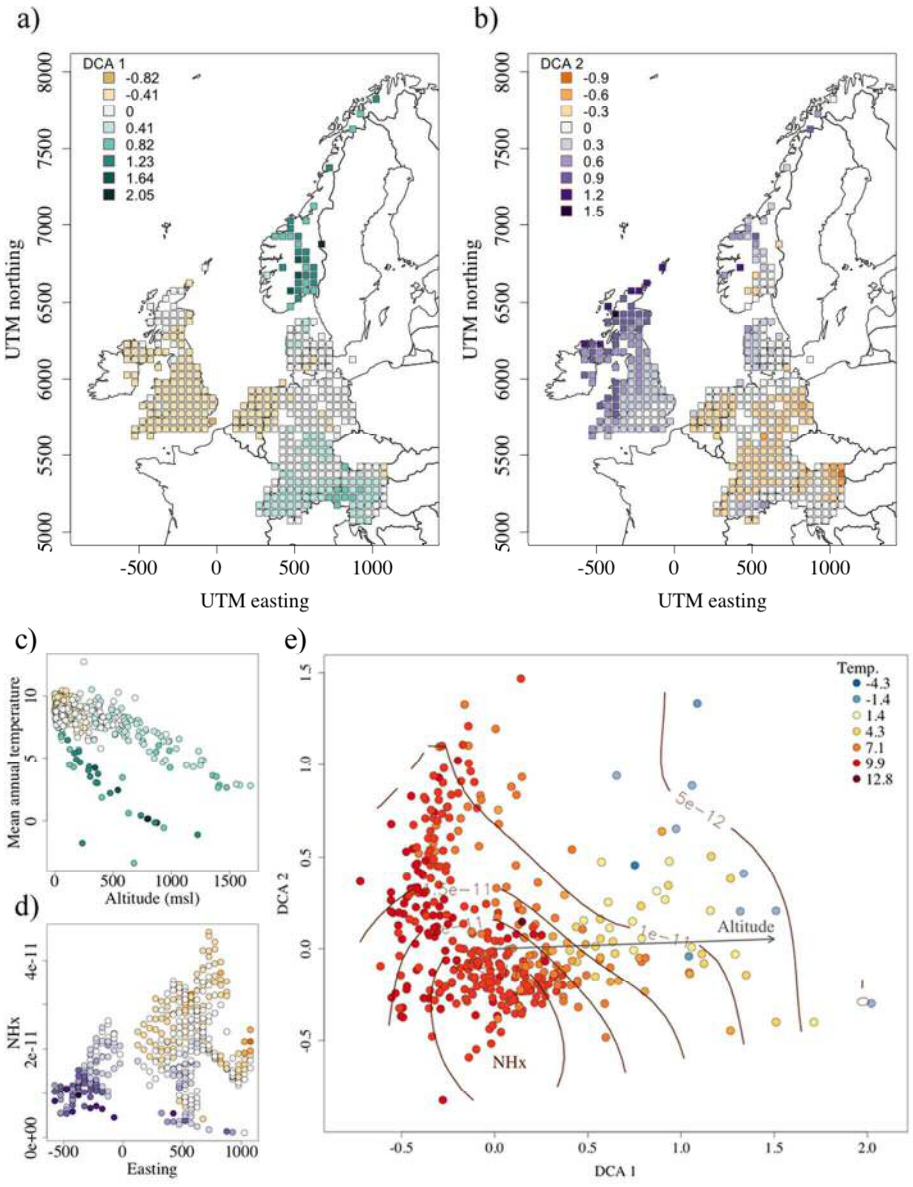


Gradients in the composition of saprotrophic fungal communities, their biogeographical distributions, and environmental correlates. Compositional similarities are represented by DCA axis 1 (a, c) and axis 2 (b, d) gradients mapped onto 50x50 km grids. Shading reflects DCA axis gradients, centered at zero (white), with darker values at either extreme. DCA plots (e) demonstrate the influence of mean annual temperature, altitude and nitrogen (NHx), all of which were highly correlated with either of the DCA axes.

400x509mm (72 x 72 DPI)

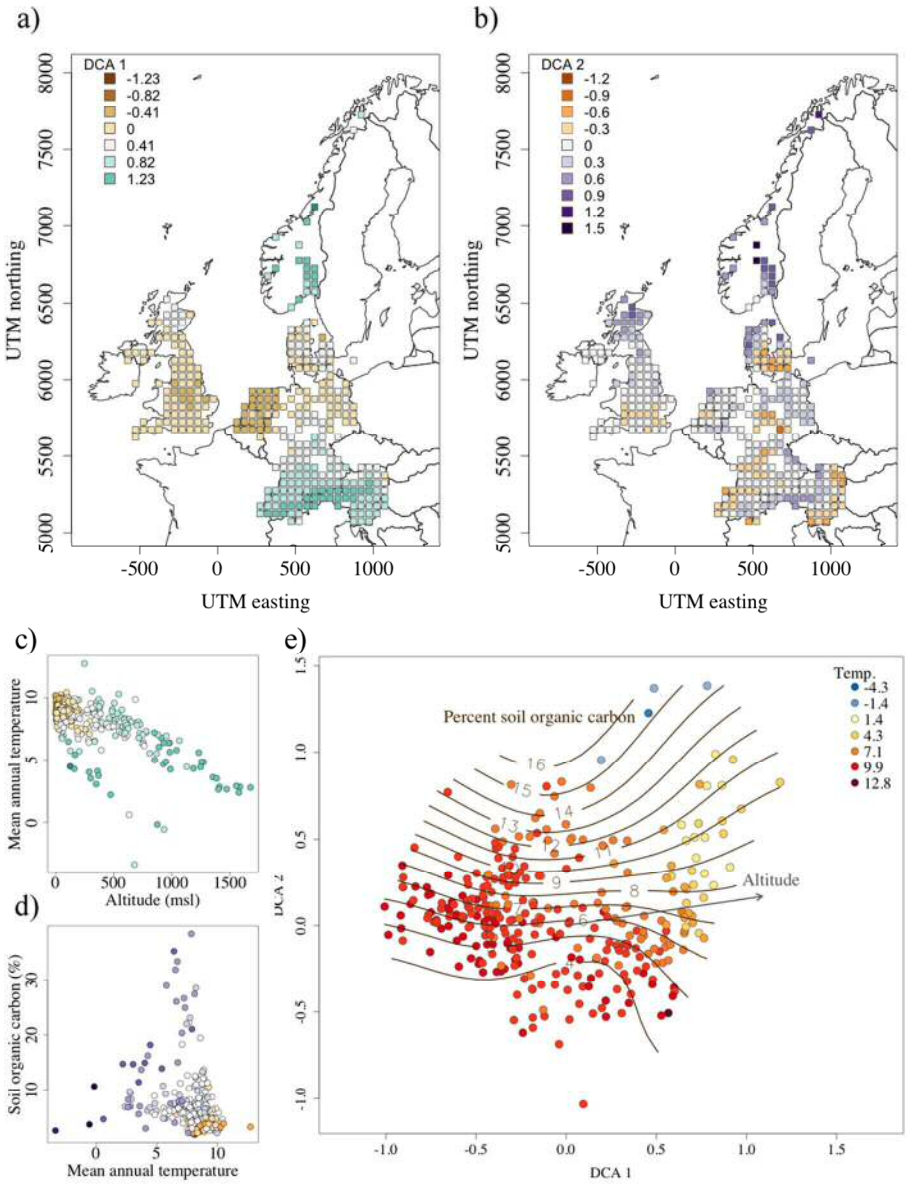


Gradients in the composition of ectomycorrhizal fungal communities, their biogeographical distributions, and environmental correlates. Compositional similarities are represented by DCA axis 1 (a, c) and axis 2 (b, d) gradients mapped onto 50 × 50 km grids. Shading reflects DCA axis gradients, centered at zero (white), with darker values at either extreme. DCA plots (e) demonstrate the influence of mean annual temperature, altitude and percent soil organic carbon, all of which were highly correlated with either of the DCA axes.

400x509mm (72 x 72 DPI)

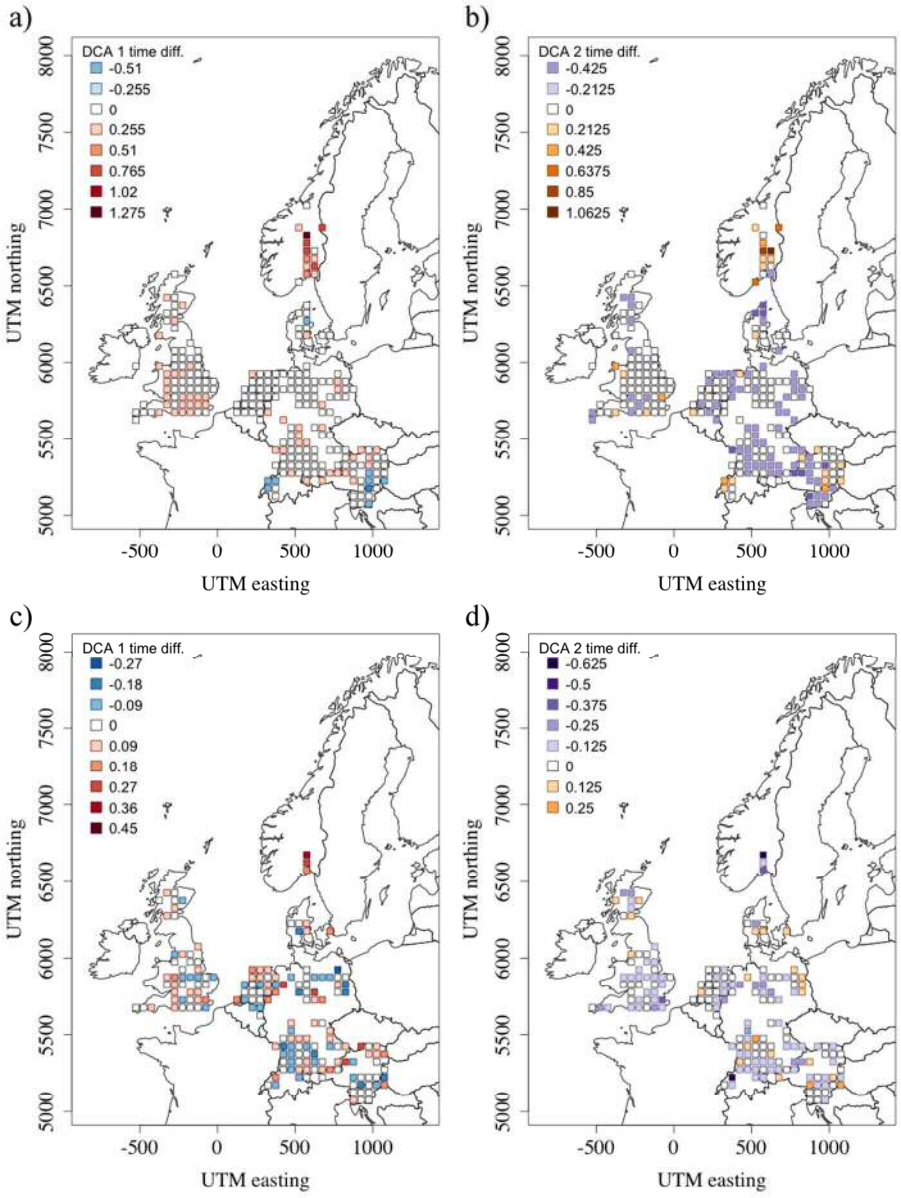


Saprotrophic (a, b) and ectomycorrhizal (c, d) fungal community differences between two time periods (1970-1990 vs. 1991-2010). The temporal differences of communities by the two main DCA gradients (t2 – t1) are shown mapped. All point shadings are centered at zero (coloured white), with shading reflecting DCA axis gradients of darker values at either extreme.

400x510mm (72 x 72 DPI)

# Continental-scale macro-fungal assemblage patterns correlate with climate, soil carbon and nitrogen deposition

Carrie Andrew, Rune Halvorsen, Einar Heegaard, Thomas W Kuyper, Jacob Heilmann-Clausen, Irmgard Krisai-Greilhuber, Claus Bässler, Simon Egli, Alan C Gange, Klaus Høiland, Paul M Kirk, Beatrice Senn-Irlet, Lynne Boddy, Ulf Büntgen, Håvard Kauserud

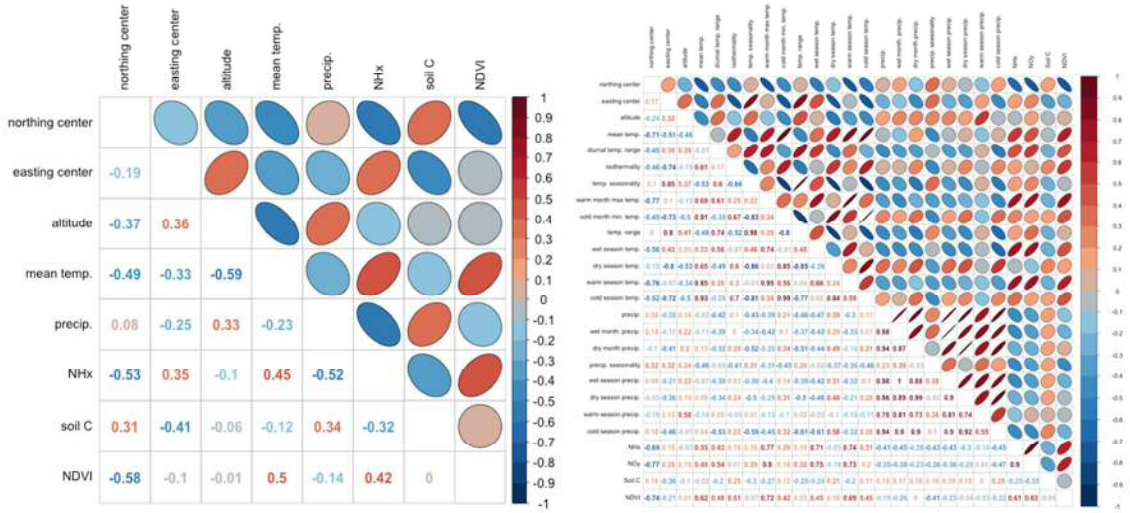


Appendix S1: Correlation plots describing collinearity between environmental variables for those selected as (a) the main variables in analyses as well as (b) all those available. The correlation values are provided in the bottom left part of the graph, while pictorial representations are found in the upper right part of the graph. Red shadings denote a positive correlation, while blue shadings denote a negative correlation. The more linear the relationships, i.e., the more the correlation approaches 1, the more linear the symbols. The less linear the relationship, i.e., the more the correlation approaches 0, the more circular the symbol shape.

# Continental-scale macro-fungal assemblage patterns correlate with climate, soil carbon and nitrogen deposition

Carrie Andrew, Rune Halvorsen, Einar Heegaard, Thomas W Kuyper, Jacob Heilmann-Clausen, Irmgard Krisai-Greilhuber, Claus Bässler, Simon Egli, Alan C Gange, Klaus Høiland, Paul M Kirk, Beatrice Senn-Irlet, Lynne Boddy, Ulf Büntgen, Håvard Kauserud

Appendix S2: Kendall tau correlations of geographical and environmental covariates with DCA axes 1, 2 and 3 for all final models: assemblages of the whole time period and divided into two time periods; all fungi, saprotrophic taxa only, and ectomycorrhizal taxa only. Values above |0.30| are in bold and those above |0.40| are shaded, signifying significantly correlated variables. The main investigated environmental correlates are in black, with medium-grey shading for additional, collinear variables. Finally, further additional WorldClim data variables that were not analysed any further (due to collinearity) are shaded the lightest-grey.

(worksheet 'AllWholeTime')

| Variable | Axis 1 | Axis 2 | Axis 3 | Variable | Axis 1 | Axis 2 | Axis 3 |
|---|---|---|---|---|---|---|---|
| Northing (grid center point) | -0.07 | **0.43** | -0.08 | prec1 | -0.08 | **0.40** | -0.17 |
| Easting (grid center point) | **0.41** | **-0.39** | 0.26 | prec2 | 0.04 | 0.29 | -0.16 |
| Altitude | **0.50** | -0.07 | 0.02 | prec3 | 0.01 | **0.30** | -0.16 |
| Temperature (annual mean) | **-0.57** | -0.16 | -0.16 | prec4 | 0.14 | 0.12 | -0.13 |
| Precipitation (annual) | 0.15 | 0.25 | -0.12 | prec5 | 0.24 | -0.06 | -0.03 |
| NHx | -0.12 | **-0.47** | 0.19 | prec6 | **0.38** | -0.16 | 0.09 |
| Soil Organic Carbon | 0.08 | 0.23 | 0.06 | prec7 | **0.43** | -0.05 | 0.13 |
| NDVI | -0.08 | -0.20 | -0.05 | prec8 | **0.34** | 0.12 | -0.02 |
| Temperature (mean diurnal range) | 0.23 | **-0.42** | 0.15 | prec9 | 0.16 | **0.34** | -0.14 |
| Isothermality (diurnal/annual ranges) | **-0.37** | 0.14 | -0.18 | prec10 | 0.05 | **0.42** | -0.19 |
| Temperature (seasonality) | **0.45** | **-0.46** | 0.22 | prec11 | 0.01 | **0.38** | -0.22 |
| Temperature (maximum of warmest month) | -0.03 | **-0.59** | 0.05 | prec12 | -0.05 | **0.37** | -0.16 |
| Temperature (minimum of coldest month) | **-0.68** | 0.20 | -0.27 | tmax1 | **-0.66** | 0.20 | -0.28 |
| Temperature range (max. warmest month - min. coldest month) | **0.45** | **-0.49** | 0.23 | tmax2 | **-0.61** | 0.07 | -0.29 |
| Temperature (mean wettest quarter) | 0.07 | **-0.53** | 0.18 | tmax3 | **-0.45** | -0.15 | -0.23 |
| Temperature (mean driest quarter) | **-0.49** | **0.33** | -0.30 | tmax4 | -0.20 | **-0.39** | -0.06 |
| Temperature (mean of warmest quarter) | -0.15 | **-0.52** | 0.03 | tmax5 | -0.12 | **-0.53** | 0.06 |
| Temperature (mean of coldest quarter) | **-0.69** | 0.18 | -0.27 | tmax6 | -0.07 | **-0.57** | 0.06 |
| Precipitation (of wettest month) | 0.27 | 0.21 | -0.10 | tmax7 | -0.03 | **-0.59** | 0.04 |
| Precipitation (of driest month) | 0.04 | 0.24 | -0.14 | tmax8 | -0.08 | **-0.58** | 0.07 |
| Precipitation seasonality coefficient of variation | **0.37** | 0.04 | 0.00 | tmax9 | -0.18 | **-0.52** | 0.04 |
| Precipitation (of wettest quarter) | 0.25 | 0.22 | -0.11 | tmax10 | **-0.45** | -0.30 | -0.08 |
| Precipitation (of driest quarter) | 0.05 | 0.24 | -0.14 | tmax11 | **-0.71** | 0.08 | -0.24 |
| Precipitation (of warmest quarter) | **0.39** | -0.02 | 0.06 | tmax12 | **-0.68** | 0.20 | -0.27 |
| Precipitation (of coldest quarter) | -0.03 | **0.34** | -0.17 | tmin1 | **-0.68** | 0.21 | -0.27 |
| NOy | -0.01 | **-0.55** | 0.26 | tmin2 | **-0.67** | 0.16 | -0.27 |
| | | | | tmin3 | **-0.68** | 0.10 | -0.25 |
| | | | | tmin4 | **-0.60** | -0.09 | -0.19 |
| | | | | tmin5 | **-0.38** | -0.29 | -0.07 |
| | | | | tmin6 | -0.29 | **-0.30** | -0.06 |
| | | | | tmin7 | -0.27 | **-0.31** | -0.06 |
| | | | | tmin8 | -0.30 | -0.28 | -0.05 |
| | | | | tmin9 | **-0.45** | -0.14 | -0.11 |
| | | | | tmin10 | **-0.60** | 0.02 | -0.17 |
| | | | | tmin11 | **-0.72** | 0.11 | -0.19 |
| | | | | tmin12 | **-0.70** | 0.22 | -0.25 |

(worksheet 'SaproWholeTime')

| Variable | Axis 1 | Axis 2 | Axis 3 | Variable | Axis 1 | Axis 2 | Axis 3 |
|---|---|---|---|---|---|---|---|
| Northing (grid center point) | -0.14 | **0.34** | **-0.43** | prec1 | -0.12 | **0.43** | -0.12 |
| Easting (grid center point) | **0.41** | **-0.43** | 0.15 | prec2 | 0.00 | **0.32** | 0.03 |
| Altitude | **0.48** | -0.05 | 0.22 | prec3 | -0.03 | **0.33** | -0.01 |
| Temperature (annual mean) | **-0.55** | -0.10 | 0.16 | prec4 | 0.12 | 0.15 | 0.19 |
| Precipitation (annual) | 0.13 | 0.27 | 0.02 | prec5 | 0.25 | -0.04 | 0.28 |
| NHx | -0.04 | **-0.49** | 0.16 | prec6 | **0.41** | -0.16 | 0.23 |
| Soil Organic Carbon | 0.13 | 0.16 | -0.16 | prec7 | **0.44** | -0.09 | 0.10 |
| NDVI | -0.02 | -0.14 | 0.21 | prec8 | **0.34** | 0.10 | 0.08 |
| Temperature (mean diurnal range) | 0.29 | **-0.39** | **0.31** | prec9 | 0.13 | **0.36** | -0.08 |
| Isothermality (diurnal/annual ranges) | **-0.36** | 0.21 | 0.05 | prec10 | 0.00 | **0.45** | -0.18 |
| Temperature (seasonality) | **0.48** | **-0.50** | 0.16 | prec11 | -0.04 | **0.43** | -0.13 |
| Temperature (maximum of warmest month) | 0.02 | **-0.56** | **0.32** | prec12 | -0.08 | **0.41** | -0.11 |
| Temperature (minimum of coldest month) | **-0.69** | 0.25 | -0.04 | tmax1 | **-0.67** | 0.28 | -0.04 |
| Temperature range (max. warmest month - min. coldest month) | **0.49** | **-0.50** | 0.18 | tmax2 | **-0.62** | 0.16 | 0.07 |
| Temperature (mean wettest quarter) | 0.14 | **-0.58** | 0.24 | tmax3 | **-0.44** | -0.08 | 0.25 |
| Temperature (mean driest quarter) | **-0.54** | **0.35** | -0.10 | tmax4 | -0.14 | **-0.35** | **0.33** |
| Temperature (mean of warmest quarter) | -0.09 | **-0.50** | 0.26 | tmax5 | -0.05 | **-0.52** | 0.30 |
| Temperature (mean of coldest quarter) | **-0.70** | 0.25 | -0.03 | tmax6 | 0.00 | **-0.55** | 0.29 |
| Precipitation (of wettest month) | 0.26 | 0.20 | 0.03 | tmax7 | 0.03 | **-0.56** | **0.32** |
| Precipitation (of driest month) | 0.02 | 0.27 | 0.07 | tmax8 | -0.02 | **-0.56** | **0.30** |
| Precipitation seasonality coefficient of variation | **0.36** | -0.03 | -0.04 | tmax9 | -0.12 | **-0.48** | **0.31** |
| Precipitation (of wettest quarter) | 0.24 | 0.21 | 0.03 | tmax10 | **-0.42** | -0.24 | 0.23 |
| Precipitation (of driest quarter) | 0.02 | 0.27 | 0.05 | tmax11 | **-0.71** | 0.17 | 0.02 |
| Precipitation (of warmest quarter) | **0.40** | -0.05 | 0.13 | tmax12 | **-0.69** | 0.28 | -0.05 |
| Precipitation (of coldest quarter) | -0.07 | **0.38** | -0.05 | tmin1 | **-0.68** | 0.27 | -0.05 |
| NOy | 0.07 | **-0.57** | 0.19 | tmin2 | **-0.68** | 0.21 | 0.00 |
| | | | | tmin3 | **-0.68** | 0.16 | 0.04 |
| | | | | tmin4 | **-0.58** | -0.03 | 0.13 |
| | | | | tmin5 | **-0.35** | -0.24 | 0.12 |
| | | | | tmin6 | -0.24 | -0.27 | 0.11 |
| | | | | tmin7 | -0.23 | -0.27 | 0.10 |
| | | | | tmin8 | -0.27 | -0.25 | 0.09 |
| | | | | tmin9 | **-0.43** | -0.09 | 0.03 |
| | | | | tmin10 | **-0.59** | 0.08 | -0.06 |
| | | | | tmin11 | **-0.71** | 0.16 | -0.05 |
| | | | | tmin12 | **-0.68** | 0.28 | -0.11 |

(worksheet 'EctoWholeTime')

| Variable | Axis 1 | Axis 2 | Axis 3 | Variable | Axis 1 | Axis 2 | Axis 3 |
|---|---|---|---|---|---|---|---|
| Northing (grid center point) | **-0.32** | **0.33** | -0.26 | prec1 | -0.06 | 0.06 | 0.13 |
| Easting (grid center point) | **0.36** | -0.05 | -0.01 | prec2 | 0.12 | 0.00 | 0.24 |
| Altitude | **0.60** | -0.04 | 0.27 | prec3 | 0.08 | 0.02 | 0.22 |
| Temperature (annual mean) | **-0.48** | -0.29 | -0.18 | prec4 | 0.29 | -0.10 | 0.28 |
| Precipitation (annual) | 0.25 | 0.03 | 0.23 | prec5 | **0.39** | -0.12 | **0.30** |
| NHx | -0.10 | -0.23 | 0.01 | prec6 | **0.47** | -0.07 | 0.27 |
| Soil Organic Carbon | 0.11 | **0.36** | 0.13 | prec7 | **0.47** | 0.03 | 0.24 |
| NDVI | 0.00 | -0.19 | 0.06 | prec8 | **0.42** | 0.07 | 0.27 |
| Temperature (mean diurnal range) | **0.32** | -0.19 | 0.13 | prec9 | 0.22 | 0.11 | 0.15 |
| Isothermality (diurnal/annual ranges) | -0.24 | -0.06 | 0.08 | prec10 | 0.07 | 0.12 | 0.04 |
| Temperature (seasonality) | **0.42** | -0.06 | -0.01 | prec11 | 0.06 | 0.05 | 0.08 |
| Temperature (maximum of warmest month) | 0.05 | **-0.35** | -0.07 | prec12 | -0.02 | 0.04 | 0.12 |
| Temperature (minimum of coldest month) | **-0.60** | -0.11 | -0.11 | tmax1 | **-0.57** | -0.13 | -0.14 |
| Temperature range (max. warmest month - min. coldest month) | **0.47** | -0.08 | 0.04 | tmax2 | **-0.47** | -0.21 | -0.10 |
| Temperature (mean wettest quarter) | 0.11 | -0.17 | -0.01 | tmax3 | -0.30 | **-0.33** | -0.09 |
| Temperature (mean driest quarter) | **-0.50** | -0.03 | -0.11 | tmax4 | -0.08 | **-0.36** | -0.07 |
| Temperature (mean of warmest quarter) | -0.09 | **-0.34** | -0.15 | tmax5 | -0.05 | **-0.33** | -0.07 |
| Temperature (mean of coldest quarter) | **-0.60** | -0.13 | -0.13 | tmax6 | 0.00 | **-0.33** | -0.10 |
| Precipitation (of wettest month) | **0.39** | 0.05 | 0.21 | tmax7 | 0.06 | **-0.35** | -0.07 |
| Precipitation (of driest month) | 0.14 | -0.03 | 0.26 | tmax8 | -0.01 | **-0.35** | -0.09 |
| Precipitation seasonality coefficient of variation | **0.38** | 0.13 | 0.02 | tmax9 | -0.09 | **-0.38** | -0.07 |
| Precipitation (of wettest quarter) | **0.37** | 0.05 | 0.22 | tmax10 | **-0.36** | **-0.35** | -0.15 |
| Precipitation (of driest quarter) | 0.13 | -0.02 | 0.26 | tmax11 | **-0.59** | -0.20 | -0.16 |
| Precipitation (of warmest quarter) | **0.46** | 0.01 | 0.27 | tmax12 | **-0.59** | -0.12 | -0.15 |
| Precipitation (of coldest quarter) | 0.01 | 0.02 | 0.17 | tmin1 | **-0.61** | -0.10 | -0.12 |
| NOy | 0.01 | -0.18 | 0.08 | tmin2 | **-0.58** | -0.14 | -0.10 |
| | | | | tmin3 | **-0.57** | -0.15 | -0.09 |
| | | | | tmin4 | **-0.50** | -0.25 | -0.16 |
| | | | | tmin5 | **-0.34** | -0.30 | -0.24 |
| | | | | tmin6 | -0.24 | -0.28 | -0.26 |
| | | | | tmin7 | -0.23 | -0.27 | -0.26 |
| | | | | tmin8 | -0.27 | -0.25 | -0.25 |
| | | | | tmin9 | **-0.42** | -0.22 | -0.22 |
| | | | | tmin10 | **-0.57** | -0.15 | -0.22 |
| | | | | tmin11 | **-0.67** | -0.12 | -0.17 |
| | | | | tmin12 | **-0.64** | -0.09 | -0.18 |

(worksheet 'EctoTwoTimePeriods')

| Variable | Axis 1 | Axis 2 | Axis 3 | Variable | Axis 1 | Axis 2 | Axis 3 |
|---|---|---|---|---|---|---|---|
| Northing (grid center point) | **-0.51** | 0.06 | 0.13 | prec1 | -0.12 | 0.02 | 0.13 |
| Easting (grid center point) | **0.41** | 0.08 | -0.12 | prec2 | 0.14 | 0.07 | 0.06 |
| Altitude | **0.69** | 0.16 | -0.07 | prec3 | 0.07 | 0.06 | 0.10 |
| Temperature (annual mean) | **-0.38** | **-0.43** | 0.12 | prec4 | **0.41** | 0.06 | 0.02 |
| Precipitation (annual) | 0.27 | 0.12 | 0.05 | prec5 | **0.53** | 0.13 | -0.04 |
| NHx | -0.08 | -0.01 | -0.19 | prec6 | **0.54** | 0.18 | -0.09 |
| Soil Organic Carbon | 0.04 | **0.37** | 0.13 | prec7 | **0.44** | 0.22 | -0.11 |
| NDVI | 0.19 | 0.01 | 0.04 | prec8 | **0.45** | 0.23 | -0.05 |
| Temperature (mean diurnal range) | **0.48** | 0.05 | -0.08 | prec9 | 0.19 | 0.10 | 0.05 |
| Isothermality (diurnal/annual ranges) | -0.24 | -0.09 | 0.12 | prec10 | 0.02 | -0.02 | 0.12 |
| Temperature (seasonality) | **0.45** | 0.11 | -0.12 | prec11 | 0.03 | -0.02 | 0.12 |
| Temperature (maximum of warmest month) | 0.26 | -0.16 | -0.03 | prec12 | -0.04 | 0.02 | 0.14 |
| Temperature (minimum of coldest month) | **-0.54** | -0.27 | 0.14 | tmax1 | -0.48 | **-0.30** | 0.14 |
| Temperature range (max. warmest month - min. coldest month) | **0.52** | 0.10 | -0.13 | tmax2 | **-0.38** | **-0.36** | 0.14 |
| Temperature (mean wettest quarter) | 0.17 | 0.01 | -0.12 | tmax3 | -0.16 | **-0.41** | 0.12 |
| Temperature (mean driest quarter) | **-0.51** | -0.19 | 0.20 | tmax4 | 0.14 | -0.23 | 0.04 |
| Temperature (mean of warmest quarter) | 0.08 | -0.25 | -0.02 | tmax5 | 0.14 | -0.16 | -0.02 |
| Temperature (mean of coldest quarter) | **-0.52** | **-0.31** | 0.15 | tmax6 | 0.18 | -0.16 | -0.02 |
| Precipitation (of wettest month) | **0.44** | 0.15 | -0.01 | tmax7 | 0.27 | -0.16 | -0.03 |
| Precipitation (of driest month) | 0.17 | 0.10 | 0.04 | tmax8 | 0.18 | -0.18 | -0.02 |
| Precipitation seasonality coefficient of variation | **0.40** | 0.16 | -0.09 | tmax9 | 0.08 | -0.24 | -0.02 |
| Precipitation (of wettest quarter) | **0.43** | 0.14 | 0.00 | tmax10 | -0.28 | **-0.45** | 0.05 |
| Precipitation (of driest quarter) | 0.14 | 0.09 | 0.05 | tmax11 | **-0.48** | **-0.38** | 0.12 |
| Precipitation (of warmest quarter) | **0.48** | 0.21 | -0.09 | tmax12 | **-0.51** | **-0.32** | 0.15 |
| Precipitation (of coldest quarter) | -0.02 | 0.03 | 0.12 | tmin1 | **-0.55** | -0.26 | 0.14 |
| NOy | -0.02 | 0.05 | -0.13 | tmin2 | **-0.51** | -0.29 | 0.12 |
| | | | | tmin3 | **-0.50** | **-0.31** | 0.16 |
| | | | | tmin4 | **-0.42** | **-0.41** | 0.12 |
| | | | | tmin5 | -0.27 | **-0.42** | 0.05 |
| | | | | tmin6 | -0.14 | **-0.37** | 0.03 |
| | | | | tmin7 | -0.14 | **-0.34** | 0.01 |
| | | | | tmin8 | -0.22 | **-0.34** | 0.03 |
| | | | | tmin9 | **-0.42** | **-0.35** | 0.06 |
| | | | | tmin10 | **-0.56** | **-0.30** | 0.07 |
| | | | | tmin11 | **-0.62** | -0.30 | 0.11 |
| | | | | tmin12 | **-0.58** | -0.29 | 0.14 |

(worksheet 'SaproTwoTimePeriods')

| Variable | Axis 1 | Axis 2 | Axis 3 | Variable | Axis 1 | Axis 2 | Axis 3 |
|---|---|---|---|---|---|---|---|
| Northing (grid center point) | -0.27 | 0.18 | **-0.45** | prec1 | -0.18 | 0.27 | -0.28 |
| Easting (grid center point) | **0.46** | **-0.32** | **0.37** | prec2 | 0.00 | 0.22 | -0.09 |
| Altitude | **0.55** | 0.08 | 0.14 | prec3 | -0.05 | 0.23 | -0.13 |
| Temperature (annual mean) | **-0.51** | -0.02 | 0.11 | prec4 | 0.19 | 0.15 | 0.11 |
| Precipitation (annual) | 0.14 | 0.15 | -0.05 | prec5 | **0.34** | -0.03 | 0.24 |
| NHx | -0.04 | **-0.37** | 0.28 | prec6 | **0.48** | -0.15 | 0.26 |
| Soil Organic Carbon | 0.21 | 0.01 | -0.22 | prec7 | **0.45** | -0.18 | 0.16 |
| NDVI | 0.11 | -0.03 | 0.13 | prec8 | **0.40** | 0.00 | 0.05 |
| Temperature (mean diurnal range) | **0.43** | -0.24 | **0.37** | prec9 | 0.15 | 0.22 | -0.19 |
| Isothermality (diurnal/annual ranges) | **-0.36** | 0.22 | -0.16 | prec10 | -0.02 | **0.31** | -0.29 |
| Temperature (seasonality) | **0.55** | **-0.31** | **0.33** | prec11 | -0.06 | 0.29 | -0.25 |
| Temperature (maximum of warmest month) | 0.15 | **-0.34** | **0.49** | prec12 | -0.12 | 0.25 | -0.23 |
| Temperature (minimum of coldest month) | **-0.67** | 0.17 | -0.15 | tmax1 | **-0.64** | 0.22 | -0.16 |
| Temperature range (max. warmest month - min. coldest month) | **0.58** | -0.30 | **0.33** | tmax2 | **-0.58** | 0.17 | -0.07 |
| Temperature (mean wettest quarter) | 0.21 | **-0.47** | **0.40** | tmax3 | **-0.36** | 0.04 | 0.15 |
| Temperature (mean driest quarter) | **-0.57** | 0.24 | -0.25 | tmax4 | 0.00 | -0.20 | **0.39** |
| Temperature (mean of warmest quarter) | 0.00 | **-0.34** | **0.45** | tmax5 | 0.07 | **-0.37** | **0.47** |
| Temperature (mean of coldest quarter) | **-0.66** | 0.18 | -0.14 | tmax6 | 0.12 | **-0.36** | **0.47** |
| Precipitation (of wettest month) | **0.32** | 0.12 | 0.00 | tmax7 | 0.16 | **-0.33** | **0.49** |
| Precipitation (of driest month) | 0.02 | 0.20 | -0.06 | tmax8 | 0.09 | **-0.37** | **0.49** |
| Precipitation seasonality coefficient of variation | **0.41** | -0.06 | 0.08 | tmax9 | -0.03 | **-0.32** | **0.43** |
| Precipitation (of wettest quarter) | **0.30** | 0.13 | 0.00 | tmax10 | **-0.40** | -0.13 | 0.20 |
| Precipitation (of driest quarter) | 0.01 | 0.19 | -0.07 | tmax11 | **-0.64** | 0.13 | -0.07 |
| Precipitation (of warmest quarter) | **0.45** | -0.12 | 0.16 | tmax12 | **-0.65** | 0.21 | -0.16 |
| Precipitation (of coldest quarter) | -0.12 | 0.24 | -0.19 | tmin1 | **-0.67** | 0.18 | -0.16 |
| NOy | 0.05 | **-0.47** | **0.34** | tmin2 | **-0.66** | 0.14 | -0.12 |
| | | | | tmin3 | **-0.65** | 0.12 | -0.07 |
| | | | | tmin4 | **-0.56** | 0.03 | 0.07 |
| | | | | tmin5 | **-0.33** | -0.16 | 0.21 |
| | | | | tmin6 | -0.20 | -0.16 | 0.24 |
| | | | | tmin7 | -0.18 | -0.17 | 0.23 |
| | | | | tmin8 | -0.25 | -0.18 | 0.22 |
| | | | | tmin9 | **-0.47** | -0.04 | 0.06 |
| | | | | tmin10 | **-0.61** | 0.05 | -0.07 |
| | | | | tmin11 | **-0.70** | 0.09 | -0.09 |
| | | | | tmin12 | **-0.67** | 0.19 | -0.17 |

# Continental-scale macro-fungal assemblage patterns correlate with climate, soil carbon and nitrogen deposition

Carrie Andrew, Rune Halvorsen, Einar Heegaard, Thomas W Kuyper, Jacob Heilmann-Clausen, Irmgard Krisai-Greilhuber, Claus Bässler, Simon Egli, Alan C Gange, Klaus Høiland, Paul M Kirk, Beatrice Senn-Irlet, Lynne Boddy, Ulf Büntgen, Håvard Kauserud

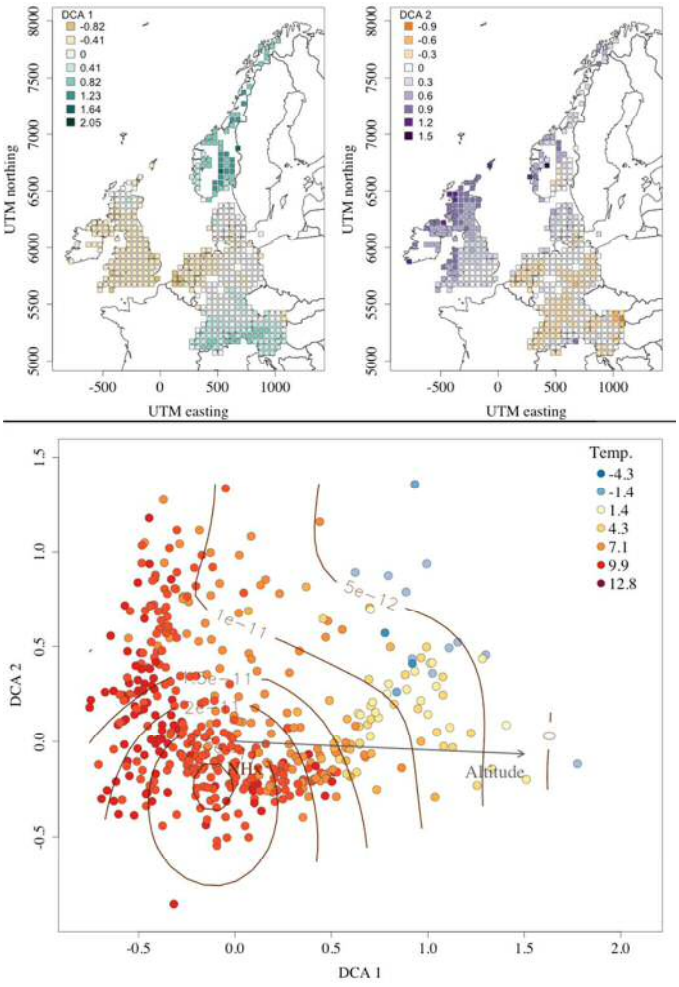


Appendix S3: Compositional gradients and biogeographic distributions of entire fungal communities (saprotrophic and ectomycorrhizal combined). Compositional similarities are represented by DCA axis 1 (a) and axis 2 (b) gradients mapped onto 50x50 km grids. Shading reflects DCA axis gradients, centered at zero (white), with darker values at either extreme. A

DCA plot (c) demonstrates the influence of mean annual temperature, altitude, and nitrogen (NHx) on fungal community gradients.

15

# Continental-scale macro-fungal assemblage patterns correlate with climate, soil carbon and nitrogen deposition

Carrie Andrew, Rune Halvorsen, Einar Heegaard, Thomas W Kuyper, Jacob Heilmann-Clausen, Irmgard Krisai-Greilhuber, Claus Bässler, Simon Egli, Alan C Gange, Klaus Høiland, Paul M Kirk, Beatrice Senn-Irlet, Lynne Boddy, Ulf Büntgen, Håvard Kauserud

Appendix S4: Output of saprotrophic indicator species analyses by fungal groups responding with positive (pos), relatively little (no), or negative (neg) change in DCA axis score(s) between the earlier (1970-1990) and later (1991-2010) time periods. The first and second worksheet ('DCA1', 'DCA2') are analyses conducted separately for each DCA axis. The third worksheet ('DCA1and2') conducts the analyses for the two DCA axes together. The keys for separation of DCA axis changes into groups is found in the first two worksheets.

(worksheet 'DCA1')

```
> summary(Indval DCA1, indvalcomp=TRUE)

 Multilevel pattern analysis
 ---------------------------

 Association function: IndVal.g
 Significance level (alpha): 0.05

 Total number of species: 3532
 Selected number of species: 50
 Number of species associated to 1 group: 49
 Number of species associated to 2 groups: 1

 List of species associated to each combination:

 Group 1  #sps.  41
                              A      B  stat p.value
Hymenochaete carpatica       0.6223 0.7778 0.696   0.002 **
Pluteus brunneoradiatus      0.9437 0.3333 0.561   0.001 ***
Clavaria versatilis          0.9274 0.3333 0.556   0.002 **
Pluteus primus               0.8974 0.3333 0.547   0.003 **
Entoloma carneogriseum       0.6958 0.3333 0.482   0.017 *
Perenniporia japonica        1.0000 0.2222 0.471   0.002 **
Volvariella cinerascens      1.0000 0.2222 0.471   0.003 **
Galerina sahleri             0.9359 0.2222 0.456   0.006 **
Agaricus abruptibulbus       0.6147 0.3333 0.453   0.010 **
Trametes quercina            0.8391 0.2222 0.432   0.015 *
Resupinatus conspersus       0.8223 0.2222 0.427   0.014 *
Lentinellus inolens          0.8041 0.2222 0.423   0.025 *
Tectella patellaris          0.7818 0.2222 0.417   0.019 *
Psilocybe turficola          0.7778 0.2222 0.416   0.016 *
Agrocybe attenuata           1.0000 0.1111 0.333   0.039 *
Asterostroma medium          1.0000 0.1111 0.333   0.039 *
Botryobasidium arachnoideum 1.0000 0.1111 0.333   0.039 *
Ceriporia rhodella           1.0000 0.1111 0.333   0.037 *
Chlorophyllum molybdites     1.0000 0.1111 0.333   0.037 *
Clavaria_sphagnicola         1.0000 0.1111 0.333   0.039 *
Cystolepiota eriophora       1.0000 0.1111 0.333   0.039 *
Fibricium subceraceum        1.0000 0.1111 0.333   0.039 *
Galerella conocephala        1.0000 0.1111 0.333   0.037 *
Mycenella variispora         1.0000 0.1111 0.333   0.039 *
Panaeolus_cyanescens         1.0000 0.1111 0.333   0.035 *
Phlebia sordida              1.0000 0.1111 0.333   0.039 *
Pholiota nameko              1.0000 0.1111 0.333   0.039 *
Psilocybe_modesta            1.0000 0.1111 0.333   0.039 *
Resupinatus striatulus       1.0000 0.1111 0.333   0.032 *
Sarcodontia_setosa           1.0000 0.1111 0.333   0.037 *
Stropharia umbonatescens     1.0000 0.1111 0.333   0.039 *
Tephrocybe raphanolens       1.0000 0.1111 0.333   0.039 *
Typhula_corallina            1.0000 0.1111 0.333   0.039 *
Galerina discreta            0.9826 0.1111 0.330   0.032 *
Kuehneromyces_vernalis       0.9826 0.1111 0.330   0.022 *
Agrocybe_farinacea           0.9741 0.1111 0.329   0.032 *
Trichaptum biforme           0.9606 0.1111 0.327   0.028 *
Auriculariopsis_albomellea   0.4753 0.2222 0.325   0.026 *
Arrhenia subglobispora       0.9494 0.1111 0.325   0.030 *
Deconica_micropora           0.9260 0.1111 0.321   0.016 *
Oudemansiella_ephippium      0.9037 0.1111 0.317   0.027 *

 Group 3  #sps.  8
                          A      B  stat p.value
Stypella_legonii        1.0000 0.1774 0.421   0.018 *
Trechispora_dimitica    0.9861 0.1613 0.399   0.023 *
Basidiodendron_spinosum 0.9646 0.1613 0.394   0.033 *
Skeletocutis_brevispora 0.9703 0.1290 0.354   0.035 *
Flaviporus_citrinellus  0.9287 0.1290 0.346   0.038 *
Radulomyces_rickii      0.9424 0.1129 0.326   0.039 *
Entoloma                0.9356 0.1129 0.325   0.029 *
Lepiota_kuehneri        0.9271 0.1129 0.324   0.046 *

 Group 1+3  #sps.  1
                          A      B  stat p.value
Mycoacia_nothofagi 0.9608 0.2254 0.465   0.029 *

### Group 1 = pos DCA1 change;  0.1275 ≤ x
### Group 2 = no DCA1 change;  -0.1275 < x < 0.1275
### Group 3 = neg DCA1 change;  x ≤ -0.1275

## "The indicator value index is the product of two components, called 'A' and 'B'.
##
##   Component 'A' is called the 'specificity' or 'positive predictive value' of the species as an indicator of the site group.
##     It is the probability that the surveyed site belongs to the target site group given the fact that the species has been found.
##     If the species has a value of 1.00, this means it occurs in sites belonging to that group only.
##
##   Component 'B' is called the 'fidelity' or 'sensitivity' of the species as indicator of the target site group.
##     It is the probability of finding the species in the sites belonging to the site group.
##     If the species has a value less than 1.00, this means not all sites belonging to that group include the species. Only the
##       proportion reported include that species.
##
```

(worksheet ‘DCA2)

```
> summary(Indval DCA2, indvalcomp=TRUE)

 Multilevel pattern analysis
 ---------------------------

 Association function: IndVal.g
 Significance level (alpha): 0.05

 Total number of species: 3532
 Selected number of species: 55
 Number of species associated to 1 group: 40
 Number of species associated to 2 groups: 15

 List of species associated to each combination:

 Group 1  #sps.  1
                    A      B  stat p.value
Pholiota pudica 0.9326 0.0641 0.245   0.037 *

 Group 3  #sps.  39
                                    A       B  stat p.value
Skeletocutis brevispora          0.92715 0.25926 0.490   0.001 ***
Skeletocutis biguttulata         0.87764 0.25926 0.477   0.001 ***
Flaviporus citrinellus           0.92741 0.22222 0.454   0.001 ***
Amylocystis lapponica            1.00000 0.18519 0.430   0.001 ***
Athelia sibirica                 1.00000 0.18519 0.430   0.001 ***
Clavaria flavipes                0.89455 0.18519 0.407   0.001 ***
Junghuhnia collabens             0.96491 0.14815 0.378   0.001 ***
Xanthoporus_syringae             0.87424 0.14815 0.360   0.003 **
Entoloma carneogriseum           0.67159 0.18519 0.353   0.010 **
Entoloma                         0.80745 0.14815 0.346   0.004 **
Athelia subovata                 1.00000 0.11111 0.333   0.002 **
Hapalopilus ochraceolateritius   1.00000 0.11111 0.333   0.004 **
Lepista regularis                1.00000 0.11111 0.333   0.001 ***
Entoloma scabropellis            0.72446 0.14815 0.328   0.014 *
Fayodia campanella               0.95238 0.11111 0.325   0.005 **
Lepista_multiformis              0.91549 0.11111 0.319   0.004 **
Antrodiella_pallasii             0.90909 0.11111 0.318   0.001 ***
Postia_lateritia                 0.90909 0.11111 0.318   0.005 **
Antrodiella_pallescens           0.88235 0.11111 0.313   0.008 **
Sistotrema raduloides            0.86379 0.11111 0.310   0.003 **
Flaviporus_americanus            0.83333 0.11111 0.304   0.008 **
Lentinellus inolens              0.71429 0.11111 0.282   0.027 *
Resupinatus_conspersus           0.67445 0.11111 0.274   0.038 *
Anomoporia_bombycina             1.00000 0.07407 0.272   0.013 *
Cabalodontia cretacea            1.00000 0.07407 0.272   0.015 *
Clavaria_pullei                  1.00000 0.07407 0.272   0.008 **
Gloeocystidiellum convolvens     1.00000 0.07407 0.272   0.014 *
Perenniporia_japonica            1.00000 0.07407 0.272   0.012 *
Pycnoporellus_alboluteus         1.00000 0.07407 0.272   0.011 *
Uncobasidium luteolum            1.00000 0.07407 0.272   0.014 *
Gloeophyllum_protractum          0.96154 0.07407 0.267   0.021 *
Skeletocutis_albocremea          0.90909 0.07407 0.259   0.020 *
Diplomitoporus_crustulinus       0.88710 0.07407 0.256   0.018 *
Antrodia_albobrunnea             0.86957 0.07407 0.254   0.022 *
Odonticium_romellii              0.85558 0.07407 0.252   0.032 *
Hyphodontia_efibulata            0.85246 0.07407 0.251   0.036 *
Laurilia_sulcata                 0.84507 0.07407 0.250   0.026 *
Phlebia_griseoflavescens         0.80082 0.07407 0.244   0.039 *
Lentaria_epichnoa                0.77458 0.07407 0.240   0.042 *

 Group 1+2  #sps.  10
                                    A      B  stat p.value
Hyphoderma_setigerum             1.0000 0.7887 0.888   0.001 ***
Botryobasidium_subcoronatum      0.9949 0.7746 0.878   0.001 ***
Cinereomyces_lindbladii          0.9837 0.6526 0.801   0.003 **
Sistotrema_brinkmannii           0.9845 0.6479 0.799   0.001 ***
Marasmiellus_vaillantii          0.9664 0.6526 0.794   0.002 **
Clitocybe_diatreta               0.9891 0.5915 0.765   0.001 ***
Pluteus_thomsonii                0.9447 0.5869 0.745   0.003 **
Crepidotus_epibryus              1.0000 0.5305 0.728   0.008 **
Hyphodontia_radula               0.9470 0.5023 0.690   0.003 **
Agrocybe_rivulosa                0.9368 0.2535 0.487   0.043 *

 Group 1+3  #sps.  3
                                   A      B  stat p.value
Mycena_strobilicola          0.91694 0.20952 0.438   0.013 *
Pluteus_primus               0.92470 0.10476 0.311   0.047 *
Agaricus_abruptibulbus       0.94235 0.09524 0.300   0.037 *

 Group 2+3  #sps.  2
                                   A      B  stat p.value
Humidicutis_calyptriformis   0.9122 0.3827 0.591   0.001 ***
Clavaria_fumosa              0.9174 0.3704 0.583   0.009 **

### Group 1 = pos DCA2 change;  0.10625 ≤ x
### Group 2 = no DCA2 change;  -0.10625 < x < 0.10625
### Group 3 = neg DCA2 change;  x ≤ -0.10625

## "The indicator value index is the product of two components, called 'A' and 'B'.
##
##   Component 'A' is called the 'specificity' or 'positive predictive value' of the species as an indicator of the site group.
##      It is the probability that the surveyed site belongs to the target site group given the fact that the species has been found.
##      If the species has a value of 1.00, this means it occurs in sites belonging to that group only.
##
##   Component 'B' is called the 'fidelity' or 'sensitivity' of the species as indicator of the target site group.
##      It is the probability of finding the species in the sites belonging to the site group.
##      If the species has a value less than 1.00, this means not all sites belonging to that group include the species. Only the
##         proportion reported include that species.
##
```

(worksheet ‘DCA1and2’)

```
> summary(Indval_DCAland2, indvalcomp=TRUE)

 Multilevel pattern analysis
 ---------------------------

 Association function: IndVal.g
 Significance level (alpha): 0.05

 Total number of species: 3532
 Selected number of species: 36
 Number of species associated to 1 group: 36
 Number of species associated to 2 groups: 0
 Number of species associated to 3 groups: 0
 Number of species associated to 4 groups: 0
 Number of species associated to 5 groups: 0
 Number of species associated to 6 groups: 0
 Number of species associated to 7 groups: 0
 Number of species associated to 8 groups: 0

 List of species associated to each combination:

 Group 1  #sps.  7
                          A      B  stat p.value
Amylocystis lapponica    0.9088 0.3077 0.529   0.044 *
Athelia sibirica         0.7292 0.3077 0.474   0.046 *
Anomoporia bombycina     1.0000 0.1538 0.392   0.021 *
Clavaria pullei          1.0000 0.1538 0.392   0.019 *
Pycnoporellus alboluteus 1.0000 0.1538 0.392   0.023 *
Uncobasidium luteolum    1.0000 0.1538 0.392   0.018 *
Gloeophyllum protractum  0.9122 0.1538 0.375   0.049 *

 Group 7  #sps.  4
                          A      B  stat p.value
Perenniporia japonica    1.0000 0.2857 0.535   0.022 *
Galerina discreta        0.9787 0.1429 0.374   0.047 *
Agrocybe farinacea       0.9683 0.1429 0.372   0.047 *
Arrhenia subglobispora 0.9386 0.1429 0.366   0.047 *

 Group 8  #sps.  5
                          A      B  stat p.value
Deconica micropora       0.9819 1.0000 0.991   0.001 ***
Antrodiella leucoxantha 0.9286 1.0000 0.964   0.020 *
Mycena juniperina        0.9242 1.0000 0.961   0.021 *
Mucronella flava         0.8861 1.0000 0.941   0.002 **
Entoloma_callichroum     0.8726 1.0000 0.934   0.032 *

 Group 9  #sps.  20
                          A      B  stat p.value
Ceriporia rhodella       1.0000 1.0000 1.000   0.008 **
Galerella_conocephala    1.0000 1.0000 1.000   0.008 **
Sarcodontia setosa       1.0000 1.0000 1.000   0.008 **
Kuehneromyces_vernalis   0.9940 1.0000 0.997   0.002 **
Delicatula_cuspidata     0.9907 1.0000 0.995   0.005 **
Trichaptum biforme       0.9889 1.0000 0.994   0.002 **
Gymnopus_exsculptus      0.9821 1.0000 0.991   0.008 **
Maireina maxima          0.9727 1.0000 0.986   0.011 *
Oudemansiella ephippium  0.9690 1.0000 0.984   0.003 **
Hymenochaete_mougeotii   0.9649 1.0000 0.982   0.009 **
Clitocybe dicolor        0.9316 1.0000 0.965   0.018 *
Clitocybe_infundibuliformis 0.9242 1.0000 0.961   0.016 *
Hygrocybe_murinacea      0.9167 1.0000 0.957   0.014 *
Crepidotus_brunneoroseus 0.9016 1.0000 0.950   0.015 *
Trametes_quercina        0.8948 1.0000 0.946   0.015 *
Volvariella_cinerascens  0.8750 1.0000 0.935   0.018 *
Pluteus_insidiosus       0.8747 1.0000 0.935   0.006 **
Pholiota_pudica          0.8730 1.0000 0.934   0.028 *
Melanoleuca_subsejuncta  0.8594 1.0000 0.927   0.023 *
Clavaria_versatilis      0.8228 1.0000 0.907   0.028 *

### Group 1 = pos DCA1, pos DCA2 change
### Group 2 = pos DCA1, neg DCA2 change
### Group 3 = pos DCA1, no DCA2 change
### Group 4 = no DCA1, pos DCA2 change
### Group 5 = no DCA1, neg DCA2 change
### Group 6 = no DCA1, no DCA2 change
### Group 7 = neg DCA1, pos DCA2 change
### Group 8 = neg DCA1, neg DCA2 change
### Group 9 = neg DCA1, no DCA2 change

## "The indicator value index is the product of two components, called 'A' and 'B'.
##
##   Component 'A' is called the 'specificity' or 'positive predictive value' of the species as an indicator of the site group.
##                 It is the probability that the surveyed site belongs to the target site group given the fact that the species has been found.
##                 If the species has a value of 1.00, this means it occurs in sites belonging to that group only.
##
##   Component 'B' is called the 'fidelity' or 'sensitivity' of the species as indicator of the target site group.
##                 It is the probability of finding the species in the sites belonging to the site group.
##                 If the species has a value less than 1.00, this means not all sites belonging to that group include the species. Only the
##                    proportion reported include that species.
##
```

# Continental-scale macro-fungal assemblage patterns correlate with climate, soil carbon and nitrogen deposition

Carrie Andrew, Rune Halvorsen, Einar Heegaard, Thomas W Kuyper, Jacob Heilmann-Clausen, Irmgard Krisai-Greilhuber, Claus Bässler, Simon Egli, Alan C Gange, Klaus Høiland, Paul M Kirk, Beatrice Senn-Irlet, Lynne Boddy, Ulf Büntgen, Håvard Kauserud

Appendix S5: Output of ectomycorrhizal indicator species analyses by fungal groups responding with positive (pos), relatively little (no), or negative (neg) change in DCA axis score(s) between the earlier (1970-1990) and later (1991-2010) time periods. The first and second worksheet ('DCA1', 'DCA2') are analyses conducted separately for each DCA axis. The third worksheet ('DCA1and2') conducts the analyses for the two DCA axes together. The keys for separation of DCA axis changes into groups is found in the first two worksheets.

(worksheet 'DCA1')

```
> summary(Indval DCA1, indvalcomp=TRUE)

 Multilevel pattern analysis
 ---------------------------

 Association function: IndVal.g
 Significance level (alpha): 0.05

 Total number of species: 2013
 Selected number of species: 9
 Number of species associated to 1 group: 5
 Number of species associated to 2 groups: 4

 List of species associated to each combination:

 Group 1  #sps.  1
                          A       B  stat p.value
Cortinarius camptoros 0.82174 0.07317 0.245   0.046 *

 Group 2  #sps.  1
                          A      B  stat p.value
Russula pseudoromellii 1.0000 0.1029 0.321   0.005 **

 Group 3  #sps.  3
                          A       B  stat p.value
Amanita betulae       1.00000 0.06349 0.252   0.035 *
Cortinarius humolens 1.00000 0.06349 0.252   0.016 *
Sarcodon lundellii    1.00000 0.06349 0.252   0.049 *

 Group 1+2  #sps.  1
                       A      B  stat p.value
Sebacina grisea 0.9173 0.4128 0.615   0.003 **

 Group 2+3  #sps.  3
                          A      B  stat p.value
Russula luteotacta 0.9914 0.5496 0.738   0.002 **
Russula subfoetens 0.9867 0.5496 0.736   0.001 ***
Phellodon niger    0.9063 0.5191 0.686   0.005 **
---

### Group 1 = pos DCA1 change;  0.045 ≤ x
### Group 2 = no DCA1 change;  -0.045 < x < 0.045
### Group 3 = neg DCA1 change;  x ≤ -0.045

## "The indicator value index is the product of two components, called 'A' and 'B'.
##
##   Component 'A' is called the 'specificity' or 'positive predictive value' of the species as an indicator of the site group.
##       It is the probability that the surveyed site belongs to the target site group given the fact that the species has been found.
##       If the species has a value of 1.00, this means it occurs in sites belonging to that group only.
##
##   Component 'B' is called the 'fidelity' or 'sensitivity' of the species as indicator of the target site group.
##       It is the probability of finding the species in the sites belonging to the site group.
##       If the species has a value less than 1.00, this means not all sites belonging to that group include the species. Only the
##           proportion reported include that species.
##
```

(worksheet ‘DCA2’)

```
> summary(Indval DCA2, indvalcomp=TRUE)

 Multilevel pattern analysis
 ---------------------------

 Association function: IndVal.g
 Significance level (alpha): 0.05

 Total number of species: 2013
 Selected number of species: 7
 Number of species associated to 1 group: 6
 Number of species associated to 2 groups: 1

 List of species associated to each combination:

 Group 1  #sps.  1
                          A       B  stat p.value
Neoboletus_pseudosulphureus 1.00000 0.07407 0.272   0.045 *

 Group 3  #sps.  5
                          A       B  stat p.value
Tomentella_atroarenicolor 0.67244 0.13636 0.303   0.042 *
Cortinarius_aquilanus     1.00000 0.09091 0.302   0.015 *
Tomentellopsis_pusilla    1.00000 0.09091 0.302   0.018 *
Russula_innocua           0.94848 0.09091 0.294   0.015 *
Hebeloma_eburneum         0.87588 0.09091 0.282   0.036 *

 Group 1+2  #sps.  1
                          A      B  stat p.value
Cortinarius_splendens 0.9660 0.3933 0.616   0.023 *
---

### Group 1 = pos DCA2 change;  0.0625 ≤ x
### Group 2 = no DCA2 change;  -0.0625 < x < 0.0625
### Group 3 = neg DCA2 change;  x ≤ -0.0625

## "The indicator value index is the product of two components, called 'A' and 'B'.
##
##   Component 'A' is called the 'specificity' or 'positive predictive value' of the species as an indicator of the site group.
##     It is the probability that the surveyed site belongs to the target site group given the fact that the species has been found.
##     If the species has a value of 1.00, this means it occurs in sites belonging to that group only.
##
##   Component 'B' is called the 'fidelity' or 'sensitivity' of the species as indicator of the target site group.
##     It is the probability of finding the species in the sites belonging to the site group.
##     If the species has a value less than 1.00, this means not all sites belonging to that group include the species. Only the
##       proportion reported include that species.
##
```

(worksheet ‘DCA1and2’)

```
> summary(Indval DCA1and2, indvalcomp=TRUE)

 Multilevel pattern analysis
 ---------------------------

 Association function: IndVal.g
 Significance level (alpha): 0.05

 Total number of species: 2013
 Selected number of species: 25
 Number of species associated to 1 group: 25
 Number of species associated to 2 groups: 0
 Number of species associated to 3 groups: 0
 Number of species associated to 4 groups: 0
 Number of species associated to 5 groups: 0
 Number of species associated to 6 groups: 0
 Number of species associated to 7 groups: 0
 Number of species associated to 8 groups: 0

 List of species associated to each combination:

 Group 1  #sps.  24
                          A      B  stat p.value
Cortinarius_aquilanus     1.0000 0.5000 0.707   0.001 ***
Paxillus_validus          0.7941 0.5000 0.630   0.001 ***
Paxillus_obscurisporus    0.7343 0.5000 0.606   0.005 **
Cortinarius_collinitoides 1.0000 0.2500 0.500   0.022 *
Cortinarius_violaceipes   1.0000 0.2500 0.500   0.022 *
Descolea_antarctica       1.0000 0.2500 0.500   0.028 *
Hebeloma_vesterholtii     1.0000 0.2500 0.500   0.022 *
Tretomyces_lutescens      1.0000 0.2500 0.500   0.028 *
Hebeloma_album            0.9444 0.2500 0.486   0.011 *
Cortinarius_pseudosalor   0.8889 0.2500 0.471   0.012 *
Cortinarius_variiformis   0.8706 0.2500 0.467   0.015 *
Cortinarius_rhizophorus   0.8621 0.2500 0.464   0.031 *
Hebeloma_quercetorum      0.8095 0.2500 0.450   0.007 **
Cortinarius_lilacinovelatus 0.8065 0.2500 0.449   0.046 *
Cortinarius_americanus    0.8003 0.2500 0.447   0.028 *
Cortinarius_multiformium  0.7931 0.2500 0.445   0.027 *
Lactarius_terenopus       0.7887 0.2500 0.444   0.030 *
Cortinarius_lepistoides   0.7576 0.2500 0.435   0.041 *
Inocybe_melanopoda        0.7368 0.2500 0.429   0.038 *
Cortinarius_tiliaceus     0.7164 0.2500 0.423   0.024 *
Cortinarius_selandicus    0.6757 0.2500 0.411   0.041 *
Tricholoma_inocyboides    0.6667 0.2500 0.408   0.031 *
Sebacina_laciniata        0.6588 0.2500 0.406   0.039 *
Ramaria_krieglsteineri    0.6538 0.2500 0.404   0.040 *

 Group 7  #sps.  1
                      A   B  stat p.value
Tomentellopsis_pusilla 1.0 0.2 0.447   0.042 *
---

### Group 1 = pos DCA1, pos DCA2 change
### Group 2 = pos DCA1, neg DCA2 change
### Group 3 = pos DCA1, no DCA2 change
### Group 4 = no DCA1, pos DCA2 change
### Group 5 = no DCA1, neg DCA2 change
### Group 6 = no DCA1, no DCA2 change
### Group 7 = neg DCA1, pos DCA2 change
### Group 8 = neg DCA1, neg DCA2 change
### Group 9 = neg DCA1, no DCA2 change

## "The indicator value index is the product of two components, called 'A' and 'B'.
##
##   Component 'A' is called the 'specificity' or 'positive predictive value' of the species as an indicator of the site group.
##     It is the probability that the surveyed site belongs to the target site group given the fact that the species has been found.
##     If the species has a value of 1.00, this means it occurs in sites belonging to that group only.
##
##   Component 'B' is called the 'fidelity' or 'sensitivity' of the species as indicator of the target site group.
##     It is the probability of finding the species in the sites belonging to the site group.
##     If the species has a value less than 1.00, this means not all sites belonging to that group include the species. Only the
##       proportion reported include that species.
##
```